

## รายงานวิจัยฉบับสมบูรณ์

โครงการ ผลของฟิสิกส์ที่ระดับพลังงานสูงต่อเอกภพที่สังเกตได้

โดย คัมภีร์ ค้าแหวน

เดือน ปี ที่เสร็จโครงการ เมษายน 2552

## สัญญาเลขที่ TRG5080012

### รายงานวิจัยฉบับสมบูรณ์

โครงการ ผลของฟิสิกส์ที่ระดับพลังงานสูงต่อเอกภพที่สังเกตได้

ผู้วิจัย คัมภีร์ ค้าแหวน สังกัด ภาควิชาฟิสิกส์ จุฬาลงกรณ์มหาวิทยาลัย

สนับสนุนโดยสำนักงานกองทุนสนับสนุนการวิจัย

(ความเห็นในรายงานนี้เป็นของผู้วิจัย สกว.ไม่จำเป็นต้องเห็นด้วยเสมอไป)

#### กิตติกรรมประกาศ

ผู้ทำวิจัยขอขอบคุณ อาจารย์ อภิสิทธ์ อึ้งกิจจานุกิจ อาจารย์ท่านอื่น ๆและนิสิตในกลุ่ม วิจัยทฤษฎีของฟิสิกส์พลังงานสูงและจักรวาลวิทยาภาควิชาฟิสิกส์คณะวิทยาศาสตร์จุฬาลงกรณ์ มหาวิทยาลัย ตลอดจนภาควิชาฟิสิกส์ คณะวิทยาศาสตร์ และ จุฬาลงกรณ์มหาวิทยาลัย ที่ให้ คำแนะนำอันเป็นประโยชน์หรือสนับสนุนการทำวิจัยนี้เป็นอย่างดี ผู้ทำวิจัยขอแสดงความขอบคุณ ต่อ อาจารย์ บุรินทร์ กำจัดภัย สำหรับความช่วยเหลือในการเป็นนักวิจัยที่ปรึกษาให้กับ โครงการวิจัยนี้และสำหรับคำแนะนำที่เป็นประโยชน์ในการทำวิจัย นอกจากนี้ผู้ทำวิจัยขอขอบคุณ อาจารย์ที่ภาควิชาฟิสิกส์มหาวิทยาลัยเกษตรศาสตร์ที่ให้การช่วยเหลือทางด้าน computer ประสิทธิภาพสูงในการทำวิจัยนี้ โดยภาควิชาฟิสิกส์คณะวิทยาศาสตร์มหาวิทยาลัยเกษตรศาสตร์ เป็นสถานที่ทำงานใหม่ของผู้ทำวิจัยและได้ทำงานวิจัยหลายส่วนที่นี้ ท้ายที่สุดผู้ทำวิจัยขอแสดง ความขอบคุณอย่างสูงต่อ สกว. ที่ให้เงินทุนสนับสนุนในการทำวิจัยนี้

Project Code: TRG5080012

Project Title: Effects of Physics at High Energy scale on the Observable Universe

Investigator: Khamphee Karwan, Department of Physics, Chulalongkorn

University

E-mail Address : pk\_karwan@yahoo.com

Project Period: 2 years

#### Abstract

We study some consequences of high energy physics on the observable universe. We are interested in two independent topics. First we consider the coincidence problem in the interacting holographic dark energy model. To alleviate the coincidence problem, we suppose that holographic dark energy has an interaction with dark matter, We analyze the cosmic evolution for this interacting dark energy model and compare the region of parameters of the interaction terms for which the cosmic evolution has an attractor within the parameter region that satisfies the observational constraints. We have shown that for holographic dark energy model, which is inspired by holographic principle in high energy theory, a general form of the interaction between holographic dark energy and dark matter can lead to alleviation of the coincidence problem for restricted range of parameters. This implies that the introduction of interaction between dark energy and dark matter in holographic dark energy model is not so effective in alleviating coincidence problem in as the usual dark energy models.

In the second topic, we consider the effects of spacetime noncommutativity on statistical properties of Cosmic Microwave Background (CMB). We investigate the primordial power spectrum of the density perturbations based on the assumption that spacetime is noncommutative in the early stage of inflation. For k-inflation model, we show that the deviation from rotational invariance of the primordial power spectrum due to spacetime noncommutativity depends on the noncommutative length scale and sound speed of inflaton. We use five-year WMAP CMB maps to constrain the contributions from spacetime noncommutativity in this power spectrum and find that the upper bound for the noncommutative length scale should be less than 10<sup>-27</sup> cm at 99.7 % confidence level.

Keywords: cosmology, interacting dark energy, noncommutative inflation, observational constraints on cosmological models

รหัสโครงการ TRG5080012

ชื่อโครงการ ผลของฟิสิกส์ที่ระดับพลังงานสูงต่อเอกภพที่สังเกตได้

ชื่อนักวิจัย คัมภีร์ ค้าแหวน ภาควิชาฟิสิกส์ จุฬาลงกรณ์มหาวิทยาลัย

E-mail Address: pk\_karwan@yahoo.com

ระยะเวลาโครงการ 2 ปี

#### บทคัดย่อ

ผู้ทำวิจัยศึกษาผลเกี่ยวเนื่องจากฟิสิกส์พลังงานสูงต่อเอกภพที่สังเกตได้ โดยมีความสนใจในสอง หัวข้อที่แตกต่างกัน ในหัวข้อแรกศึกษาปัญหา coincidence ในแบบจำลอง holographic ของ พลังงานมืด เพื่อแก้ปัญหา coincidence จึงสมมุติว่าพลังงานมืดมีอันตรกิริยากับสสารมืด เมื่อ วิเคราะห์การวิวัฒน์ของเอกภพในกรณีนี้แล้วเปรียบเทียบช่วงของ parameter ของอันตรกิริยาที่ ทำให้การวิวัฒน์ของเอกภพมีจุดดูด กล่าวคือเกิดการแก้ปัญหา coincidence กับช่วงของ parameter ที่สอดคล้องกับข้อมูลจากการสังเกตการณ์ พบว่าในกรณีของแบบจำลองพลังงานมืดนี้ อันตรกิริยาระหว่างพลังงานมืดและสสารมืดที่มีรูปแบบทั่วไปทำให้เกิดการแก้ปัญหา coincidence ได้สำหรับช่วงแคบ ๆของ parameter เท่านั้น นี่แสดงว่าในกรณีของแบบจำลองพลังงานมืดนี้การ สมมุติว่าพลังงานมืดและสสารมืดมีอันตรกิริยากันไม่ช่วยแก้ปัญหา coincidence ได้อย่างดีเหมือน แบบจำลองพลังงานมืดหัวไป

ในหัวข้อที่สองผู้ทำวิจัยศึกษาผลของการไม่ commute กันของกาลอวกาศต่อสมบัติเชิง สถิติของ Cosmic Microwave Background (CMB) โดยใช้สมมุติฐานว่ามีการไม่ commute กัน ของกาลอวกาศในช่วงแรกของ inflation ในเอกภพยุคเริ่มต้นแล้วคำนวณหา power spectrum ของความผันผวนในการกระจายตัวของสสารและพลังงานในเอกภพยุคนี้ สำหรับกรณีของ แบบจำลอง k-inflation ผลจากการคำนวณแสดงให้เห็นว่าการเบี่ยงเบนจากการมีสมมาตรในการ หมุนของ power spectrum อันเป็นผลมาจากการไม่ commute กันของกาลอวกาศขึ้นกับ noncommutative length scale และ sound speed ของinflaton นอกจากนี้เมื่อใช้แผนที่ CMB จากผลห้าปีของ WMAP มาจำกัดปริมาณความไม่ commute กันของกาลอวกาศใน power spectrum พบว่า noncommutative length scale ควรมีค่าไม่เกิน 10<sup>-27</sup> ซม. ที่ระดับความเชื่อมั่น 99.7 %

คำหลัก จักรวาลวิทยา อันตรกิริยาระหว่างพลังงานมืดและสสารมืด การไม่ commute กันของกาล อวกาศในแบบจำลอง inflation การใช้ข้อมูลจากการสังเกตการณ์เพื่อจำกัดรูปแบบของ แบบจำลองเอกภพ จากการสังเกตการณ์ทางฟิสิกส์ดาราศาสตร์ที่มีความแม่นยำมากขึ้นในปัจจุบันทำให้เรามี ข้อมูลและรู้ถึงสมบัติของเอกภพมากขึ้น สมบัติของเอกภพที่กล่าวถึงนี้เป็นสมบัติของเอกภพที่ สังเกตได้ (observable universe) [1] เนื่องจากการเคลื่อนที่ของสสารพลังงานตลอดจนข้อมูลใน อวกาศไม่สามารถมีความเร็วเกินกว่าความเร็วของแสงในสูญญูกาศดังนั้นส่วนของเอกภพที่แสงใช้ เวลานานกว่าอายุของเอกภพในการเดินทางจากส่วนนั้นมาถึงเราจึงถูกตัดขาดจากเราและเอกภพ ในส่วนที่เราสังเกตได้ก็เป็นส่วนของเอกภพที่แสงจากส่วนนั้นสามารถเดินทางมาถึงเราได้ ในยุค เริ่มตันของเอกภพความหนาแน่นของสสารและพลังงานจะมีค่าสูงมากปรากฏการณ์ทางฟิสิกส์ที่ เกิดในเอกภพยุคนี้จึงเป็นไปตามทฤษฎีของฟิสิกส์พลังงานสูงซึ่งเป็นที่เชื่อกันโดยทั่วไปว่า ปรากฏการณ์เหล่านี้อาจทิ้งร่องรอยหรือผลพวงบางอย่างในเอกภพที่สังเกตได้ [2] ดังนั้น การศึกษาเอกภพจึงอาจช่วยให้เข้าใจหรือช่วยทดสอบทฤษฎีของฟิสิกส์พลังงานสูงในบางประเด็น ได้ซึ่งในโครงการวิจัยนี้จะศึกษาผลของปรากฏการณ์ทางฟิสิกส์พลังงานสูงบางอย่างที่มีต่อเอกภพ ที่สังเกตได้

ประเด็นหนึ่งที่ศึกษาในโครงการนี้คือศึกษาว่าปัญหา coincidence ในแบบจำลอง holographic ของพลังงานมืดซึ่งเป็นแบบจำลองที่สร้างจากสมมติฐานในฟิสิกส์พลังงานสูง [3] สามารถถูกแก้ไขได้ดีเพียงใดด้วยการสมมุติว่าพลังงานมืดมีอันตรกิริยากับสสารมืด โดยทั่วไป ปัญหาสำคัญหนึ่งของแบบจำลองพลังงานมืดซึ่งเป็นแบบจำลองที่ใช้อธิบายการขยายตัวด้วย ความเร่งในยุคปัจจุบันของเอกภพคือปัญหา coincidence [4] ซึ่งเป็นปัญหาที่ว่าเพราะสาเหตุใด ความหนาแน่นพลังงานของสสารมืดและพลังงานมืดจึงมีค่าอยู่ในระดับเดียวกัน ณ เวลาปัจจุบัน ทั้งที่ความหนาแน่นพลังงานของสสารมืดและพลังงานมืดจึงมีค่าอย่าแก่กันเมื่อเอกภพวิวัฒน์ในเวลา นั่นคือความหนาแน่นพลังงานของสสารมืดมีค่ามากกว่าความหนาแน่นพลังงานของพลังงานมืด มากในอดีตและเป็นไปในทางกลับกันในอนาคต แนวทางหนึ่งที่ช่วยแก้ปัญหา coincidence ได้ดี ในระดับหนึ่งสำหรับแบบจำลองพลังงานมืดทั่วไปคือการสมมุติว่าสสารมืดและพลังงานมืดมีอันตร กิริยากัน [5] แต่จากการศึกษาแบบจำลอง holographic ของพลังงานมืดในโครงการนี้พบว่าการ สมมุติให้สสารมืดและพลังงานมืดมีอันตรกิริยากันช่วยแก้ปัญหา coincidence ได้ไม่ดีนัก

อีกประเด็นหนึ่งที่ศึกษาในโครงการคือศึกษาว่าการไม่ commute กันของกาลอวกาศใน เอกภพยุคเริ่มต้นมีผลมากน้อยเพียงใดต่อสมบัติเชิงสถิติของ CMB และค่าที่สอดคล้องกับข้อมูล จากการวัด CMB ของ parameter ที่เกี่ยวข้องกับการไม่ commute กันของกาลอวกาศควรเป็น เช่นใด ในช่วงเริ่มต้นของยุค inflation ซึ่งเป็นส่วนหนึ่งของเอกภพยุคเริ่มต้นความหนาแน่น พลังงานของเอกภพอาจมีค่าเข้าใกลัสเกล Planck [6] อันจะทำให้มีผลจากฟิสิกส์ที่ระดับสเกล Planck ปรากฏในสมบัติของความผันผวนในการกระจายตัวของสสารและพลังงานในเอกภพ ปรากฏการณ์ทางฟิสิกส์ที่ระดับสเกล Planck ที่ศึกษาในโครงการนี้คือปรากฏการณ์ของการไม่ commute กันของกาลอวกาศอันเป็นผลมาจากธรรมชาติ quantum ของความโน้มถ่วง [7 - 8] จาการศึกษาที่เคยมีมาแสดงให้เห็นว่าการไม่ commute กันของกาลอวกาศสามารถทำให้ power

spectrum ของความผันผวนในการกระจายตัวของสสารและพลังงานเสียสมมาตรในการหมุน [9] ซึ่งจะทำให้สถิติของ CMB ไม่ isotropic [10] จากการศึกษาในโครงการพบว่าการไม่ isotropic ของสถิติของ CMB อันเป็นผลมาจากการไม่ commute กันของกาลอวกาศสามารถตรวจพบได้ จากการวิเคราะห์แผนที่ของ CMB แต่ข้อมูลของ CMB ในปัจจุบันยังมีความละเอียดไม่พอที่จะใช้ ทดสอบว่ามีการไม่ commute ของกาลอวกาศในเอกภพยุคเริ่มตันหรือไม่ อย่างไรก็ตามข้อมูลของ CMB ก็สามารถใช้จำกัดค่า parameter ที่เกี่ยวข้องกับการไม่ commute กันของกาลอวกาศได้ดี

#### 2. วิธีดำเนินการ

- 2.1 วิธีดำเนินการสำหรับการศึกษาปัญหา coincidence ในแบบจำลอง holographic ของพลังงาน มืด
- 2.1.1 คำนวณหาสมการ autonomous ที่บรรยายการวิวัฒน์ของการแผ่รังสี สสารมืด baryon และ พลังงานมืดแบบ holographic ในเอกภพ โดยสมมุติว่าพลังงานมืดและสสารมืดมีอันตรกิริยากัน
- 2.1.2 หาจุด fixed ของสมการข้างต้นและวิเคราะห์ความเสถียรของจุดเหล่านี้ ซึ่งช่วงของ parameter ของอันตรกิริยาที่ทำให้เกิดจุด fixed ที่เสถียรจะเป็นช่วงของ parameter ที่อาจทำให้ เกิดการแก้ปัญหา coincidence ได้
- 2.1.3 หาช่วงของ parameter ของอันตรกิริยาที่สอดคล้องกับข้อมูลจากการสังเกตการณ์
- 2.1.4 เปรียบเทียบช่วงของ parameter จากข้อ 2.1.2 และ 2.1.3 เพื่อพิจาณาว่าอันตรกิริยา ระหว่างสสารมืดและพลังงานมืดช่วยแก้ปัญหา coincidence ได้ดีเพียงใด
- 2.2 วิธีดำเนินการสำหรับการศึกษาผลของการไม่ commute ของกาลอวกาศต่อสมบัติเชิงสถิติ ของ CMB
- 2.2.1 คำนวณหา power spectrum ของความผันผวนในการกระจายตัวของสสารและพลังงานโดย ใช้แบบจำลอง k-inflation และสมมุติฐานที่ว่ากาลอวกาศในยุคเริ่มต้นของเอกภพไม่ commute กัน 2.2.2 คำนวณหา covariance matrix ของ สัมประสิทธิ์ของการกระจาย harmonic ของความผัน ผวนในอุณหภูมิของ CMB จาก power spectrum ข้างต้น
- 2.2.3 ตรวจสอบว่าการไม่ commute กันของกาลอวกาศที่ปรากฏใน covariance matrix ทำให้ เกิดผลที่วัดได้หรือไม่ในแผนที่ CMB และใช้แผนที่ CMB จากผลห้าปีของ WMAP [11] เพื่อจำกัด ค่าของ parameter ที่เกี่ยวข้องกับการไม่ commute กันของกาลอวกาศ

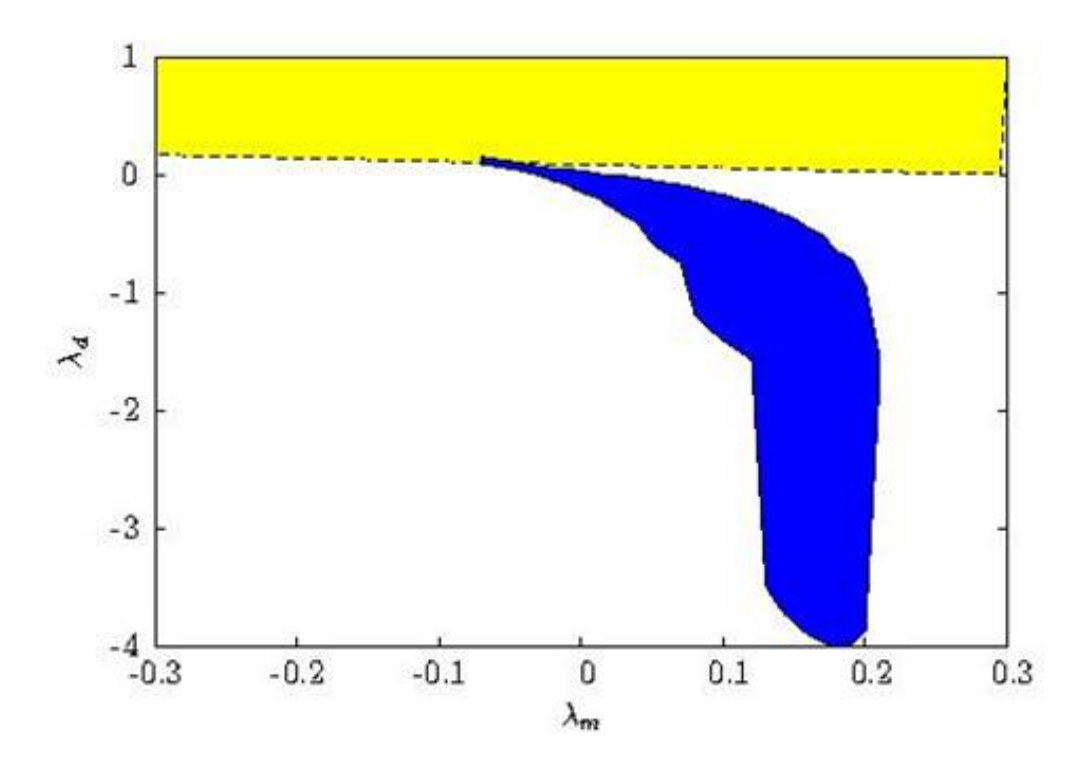
#### 3. ผลที่ได้

3.1 ผลจากการศึกษาปัญหา coincidence ในแบบจำลอง holographic ของพลังงานมืด 3.1.1 รูปแบบทั่วไปหนึ่งของอันตรกิริยาระหว่างสสารมืดและพลังงานมืดบรรยายได้ด้วยสมการ  $Q=3H(\lambda_d\rho_d+\lambda_c\rho_c)$  โดย  $\rho_d$ ,  $\rho_c$  คือความหนาแน่นพลังงานของพลังงานมืดและสสารมืด H คือ Hubble parameter และ  $\lambda_d$ ,  $\lambda_c$  คือ parameter ของอันตรกิริยา ช่วงของ parameter ที่ทำให้เกิดจุด fixed ที่เสถียรคือ

$$\lambda_d \Omega_d + \lambda_c \Omega_c > \Omega_c / 3 \tag{1}$$

โดย  $\Omega_c$  ,  $\Omega_d$  คืออัตราส่วนของความหนาแน่นพลังงานของสสารมืดและพลังงานมืดต่อพลังงาน วิกฤติที่เวลาปัจจุบัน

3.1.2 ช่วงของ parameter ที่สอดคล้องกับข้อมูลจาการสังเกตการณ์คือพื้นที่สีฟ้าในรูปที่ 1 3.1.3 ช่วงของ parameter ที่ทำให้เกิดการแก้ปัญหา coincidence คือช่วงของ parameter ที่อยู่ใน บริเวณที่พื้นที่สีฟ้าทับกับพื้นที่สีเหลือง โดยพื้นที่สีเหลืองคือช่วงของ parameter ที่สอดคล้องกับ สมการ 1



รูป 1 รูปแสดงช่วงของ parameter ของอันตรกิริยาที่ทำให้เกิดการแก้ปัญหา coincidence โดย พื้นที่สีฟ้าแสดงช่วงของ parameter ที่สอดคล้องกับข้อมูลจากการสังเกตการณ์และพื้นที่สีเหลือง แสดงช่วงของ parameter ที่สอดคล้องกับสมการ 1 ในรูปนี้ใช้ค่า  $\Omega_c=0.27$  และ  $\Omega_d=0.73$  ซึ่ง สอดคล้องกับข้อมูลจากการสังเกตการณ์

จากรูปจะเห็นได้ว่าในกรณีที่พิจารณานี้ปัญหา coincidence สามารถถูกแก้ได้สำหรับช่วงแคบ ๆ ของ parameter เท่านั้นซึ่งแสดงให้เห็นว่าปัญหา coincidence ถูกแก้ได้ไม่ดีนัก 3.2 ผลจากการศึกษาผลของการไม่ commute ของกาลอวกาศต่อสมบัติเชิงสถิติของ CMB
3.2.1 โดยการใช้สมมติฐานว่ามีการไม่ commute กันของกาลอวกาศในยุคเริ่มต้นของ inflation จะ ได้ว่า power spectrum ของความผันผวนในการกระจายตัวของสสารและพลังงานสำหรับ แบบจำลอง k-inflation สามารถเขียนในรูป

$$P(\vec{k}) = P(k) \left( 1 - v \frac{H^4 L_s^4}{c_s^2} \sin^2 o \right)$$
 (2)

โดย P(k) คือ power spectrum ของความผันผวนในกรณีที่กาลอวกาศ commute กัน  $L_s$  คือ noncommutative length scale  $c_s$  คือ sound speed ของ inflaton  $\nu$  คือ parameter ที่ เกี่ยวข้องกับอัตราเร็วในการขยายตัวของเอกภพ  $\vec{k}$  คือเวคเตอร์ของเลขคลื่นของความผันผวนใน Fourier space และ o แสดงมุมระหวังเวคเตอร์  $\vec{k}$  กับ basis ที่สามของมัน  $k_s$  พจน์ที่ สองในวงเล็บทางด้านขวามือของสมการข้างต้นเกิดจากการไม่ commute กันของกาลอวกาศซึ่ง พจน์นี้ทำให้ power spectrum ทางด้านซ้ายมือขึ้นกับทิศทางของเวคเตอร์  $\vec{k}$  นั่นคือการไม่ commute กันของกาลอวกาศทำให้ power spectrum เสียสมมาตรในการหมุน 3.2.2 เพื่อความสะดวกในการศึกษาเชิงทฤษฎีเราเขียนความผันผวนในอุณหภูมิของ CMB ในรูป ของการกระจาย harmonic

$$\Delta_T = T(\hat{n}) - T_0 = \sum_{l,m} a_{lm} Y_{lm}(\hat{n})$$
 (3)

โดย  $T(\hat{n})$  คืออุณหภูมิที่วัดในทิศทาง  $\hat{n}$   $T_0$  คืออุณหภูมิเฉลี่ยและ  $Y_{lm}(\hat{n})$  คือ spherical harmonic functions ความผันผวนในอุณหภูมิ เป็นตัวแปรสุ่มซึ่งสมบัติเชิงสถิติบรรยายได้ด้วย correlation function ใน harmonic space two-point correlation function ของความผันผวนใน อุณหภูมิขึ้นกับ covariance matrix ของ  $a_{lm}$  โดยการใช้ power spectrum ในสมการ 2 covariance matrix ของ lm เขียนได้ดังสมการ

$$\langle a_{lm} a_{l'm'}^* \rangle = \delta_{ll'} \delta_{mm'} C_l + \text{off diagonal elements}$$
 (4)

โดย  $C_l$  คือ angular power spectrum ของ CMB ในกรณีที่ power spectrum ในสมการ 2 มี สมมาตรในการหมุนกล่าวคือพจน์ที่มาจากการไม่ commute กันของกาลอวกาศเป็นศูนย์ covariance matrix จะมีเฉพาะ diagonal elements และขึ้นกับ  $C_l$  เท่านั้น การที่ covariance matrix ของ  $a_{lm}$  มี off-diagonal elements แสดงให้เห็นว่า two-point correlation function ของ  $\Delta T$  ขึ้นกับทิศทางนั่นคือสถิติของ CMB ไม่ isotropic

3.2.3 จากการวิเคราะห์แผนที่ CMB จากผลห้าปีของ WMAP แสดงให้เห็นว่าการไม่ isotropic ใน สถิติของ CMB ต้องมีค่าจำกัดด้วยเหตุนี้ noncommutative length scale ควรมีค่าไม่เกิน 10<sup>-27</sup> cm ที่ระดับความเชื่อมั่น 99.7%

#### 4. สรุป

โดยทั่วไปปัญหา coincidence ในแบบจำลองพลังงานมืดสามารถถูกแก้ได้ด้วนการสมมุติ ว่ามีอันตรกิริยากันระหว่างสสารมืดและพลังงานมืดแต่จากการศึกษาแบบจำลอง holographic ของพลังงานมืดพบว่าอันตรกิริยาระหว่างสสารมืดและพลังงานมืดช่วยแก้ปัญหา coincidence ใน แบบจำลองพลังงานมืดนี้ได้ไม่ดีนัก อย่างไรก็ตามผู้ทำวิจัยเชื่อว่าถ้าปรับปรุงรูปแบบของอันตร กิริยาอย่างเหมาะสมปัญหา coincidence อาจถูกแก้ได้ดีขึ้น

การไม่ commute กันของกาลอวกาศซึ่งเป็นผลมาจากธรรมชาติ quantum ของความโน้ม ถ่วงในเอกภพยุคเริ่มต้นสามารถทำให้เกิดผลที่วัดได้ใน CMB และโดยการวิเคราะห์แผนที่ CMB จากผลห้าปีของ WMAP พบว่า noncommutative length scale ควรมีค่าไม่เกิน 10<sup>-27</sup> ซม. ที่ ระดับความเชื่อมั่น 99.7% สำหรับแบบจำลอง k-inflation ซึ่งเป็นแบบจำลองทั่วไปของ inflation

#### หนังสืออ้างอิง

- [1] D. H. Lyth and A. Riotto, "Particle physics models of inflation and the cosmological density perturbation," Phys. Rept. **314** (1999) 1, [arXiv:hep-ph/9807278].
- [2] R. H. Brandenberger and J. Martin, ``The Robustness of inflation to changes in superPlanck scale physics," Mod. Phys. Lett. **A16** (2001) 999, [arXiv:astro-ph/0005432].
- [3] M. Li, "A Model of holographic dark energy," Phys. Lett. **B603** (2004) 1, [arXiv:hep-th/0403127].
- [4] W. Zimdahl and D. Pavon, ``Scaling cosmology," Gen. Rel. Grav. **35** (2003) 413, [arXiv:astro-ph/0210484].
- [5] H. M. Sadjadi and M. Alimohammadi, "Cosmological coincidence problem in interactive dark energy models," Phys. Rev. **D74** (2006) 103007, [arXiv:gr-qc/0610080].
- [6] S. Tsujikawa, R. Maartens and R. Brandenberger, "Noncommutative inflation," Phys. Lett. **B574** (2003) 141, [arXiv:astro-ph/0308169].
- [7] R. Brandenberger and Pei-Ming Ho, "Noncommutative space-time, stringy space-time uncertainty principle, and density fluctuations," Phys. Rev. **D66** (2002) 023517, [arXiv:hep-th/0203119].
- [8] R. J. Szabo, "Quantum field theory on noncommutative spaces," Phys. Rept. **378** (2003) 207, [arXiv:hep-th/0109162].
- [9] F. Lizzi, G. Mangano, G. Miele and M. Peloso, "Cosmological perturbations and short distance physics from noncommutative geometry," JHEP **0206** (2002) 049, [arXiv:hep-th/0203099].

[10] L. Ackerman, S. M. Carroll and M. B. Wise, "Imprints of a Primordial Preferred Direction on the Microwave Background," Phys. Rev. **D75** (2007) 083502, [arXiv:astro-ph/0701357].

[11] G. Hinshaw et al. (WMAP Collaboration), "Five-Year Wilkinson Microwave Anisotropy Probe (WMAP) Observations: Data Processing, Sky Maps, and Basic Results," Astrophys. J. Suppl. 180 (2009) 225, [arXiv:0803.0732].

#### Output

ผลงานตีพิมพ์ในวารสารวิชาการนานาชาติ

- 1. K. Karwan, ``The coincidence problem and interacting holographic dark energy," JCAP **0805** (2008) 011, [arXiv:0801.1755].
- 2. K. Karwan, "CMB constraints on spacetime noncommutativity in inflationary scenario," submitted to JCAP, [arXiv:0903.2806].

#### ภาคผนวก

- 1. รายงานการวิจัยที่ได้ตีพิมพ์ที่ JCAP
- 2. รายงานการวิจัยที่ส่งไปตีพิมพ์ที่ JCAP

# The coincidence problem and interacting holographic dark energy

#### Khamphee Karwan

Theoretical High-Energy Physics and Cosmology Group, Department of Physics, Chulalongkorn University, Bangkok 10330, Thailand E-mail: pk\_karwan@vahoo.com

Received 18 January 2008 Accepted 22 April 2008 Published 13 May 2008

Online at stacks.iop.org/JCAP/2008/i=05/a=011 doi:10.1088/1475-7516/2008/05/011

**Abstract.** We study the dynamical behaviour of the interacting holographic dark energy model whose interaction term is  $Q = 3H(\lambda_{\rm d}\rho_{\rm d} + \lambda_{\rm c}\rho_{\rm c})$ , where  $\rho_{\rm d}$  and  $\rho_{\rm c}$  are the energy densities of dark energy and cold dark matter respectively. To satisfy the observational constraints from type Ia supernovae, the cosmic microwave background shift parameter and baryon acoustic oscillation measurements, if  $\lambda_{\rm c} = \lambda_{\rm d}$  or  $\lambda_{\rm d}, \lambda_{\rm c} > 0$ , the cosmic evolution will only reach the attractor in the future and the ratio  $\rho_{\rm c}/\rho_{\rm d}$  cannot be slowly varying at present. Since the cosmic attractor can be reached in the future even when the present values of the cosmological parameters do not satisfy the observational constraints, the coincidence problem is not really alleviated in this case. However, if  $\lambda_{\rm c} \neq \lambda_{\rm d}$  and they are allowed to be negative, the ratio  $\rho_{\rm c}/\rho_{\rm d}$  can be slowly varying at present and the cosmic attractor can be reached near the present epoch. Hence, the alleviation of the coincidence problem in this case is still attainable when confronting this model with Sloan Digital Sky Survey data.

**Keywords:** dark energy theory, classical tests of cosmology

**ArXiv ePrint:** 0801.1755

Co	Contents			
1.	Introduction	2		
<b>2</b> .	The autonomous equations	3		
<b>3.</b>	The attractor of cosmic evolution	6		
4.	The observational constraints	8		
<b>5.</b>	Conclusions	14		
	Acknowledgments	15		
	References	16		

#### 1. Introduction

Observations suggest that the expansion of the universe is accelerating [1,2]. The acceleration of the universe may be explained by supposing that the present universe is dominated by a mysterious form of energy whose pressure is negative, known as dark energy. One of the weaknesses of the dark energy model is the coincidence problem, which is the problem why the dark energy density and matter density are of the same order of magnitude in the present epoch although they evolve differently during the expansion of the universe. A possible way to alleviate the coincidence problem is to suppose that there is an interaction between matter and dark energy. The cosmic coincidence can then be alleviated by appropriate choice of the form of the interaction between matter and dark energy leading to a nearly constant ratio  $r = \rho_c/\rho_d$  during the present epoch [3]–[5] or giving rise to an attractor of the cosmic evolution at late time [6,7]. Since the existence of the cosmic attractor implies constant r but the attractor does not always occur at the present epoch, we first find a range of dark energy parameters for which the attractor occurs and then check the evolution of r during the present epoch.

On the basis of holographic ideas [8,9], one can determine the dark energy density in terms of the horizon radius of the universe. This type of dark energy is holographic dark energy [10]–[14]. Choosing the Hubble radius as the cosmological horizon, the present amount of dark energy density agrees with observations. Nevertheless, dark energy evolves like matter at present, so it cannot lead to an accelerated expansion. However, if the particle horizon is chosen to be the cosmological horizon, the equation of state parameter of dark energy can become negative but not negative enough to drive an accelerating universe. The situation is better when one uses the event horizon as the cosmological horizon. In this case, dark energy can drive the present accelerated expansion, and the coincidence problem can be resolved by assuming an appropriate number of e-foldings of inflation. Roughly speaking, the coincidence problem can be resolved because the size of the cosmological horizon during the present epoch depends on the amount of e-folds of inflation, and the amount of holographic dark energy depends on the horizon size. Nevertheless, the second law of thermodynamics will be violated if  $w_d < -1$  [9,15]. Hence,  $w_d$  should not cross the boundary  $w_d = -1$ . The boundary  $w_d = -1$  can be

crossed if dark energy interacts with matter. Since now the horizon size has a dependence on the interaction terms, the alleviation of cosmic coincidence should also depend on the interaction term.

In this work we suppose that the holographic dark energy interacts only with cold dark matter (CDM) and treat baryons as non-interacting matter components. Our objective is to compare the region of dark energy parameters for which the cosmic evolution has an attractor within the parameter region that satisfies the observational constraints from combined analysis of SNIa data [16], the CMB shift parameter [17] and BAO measurements [18]. The results of the comparison can tell us about the range of parameters that alleviate the cosmic coincidence.

#### 2. The autonomous equations

In this section, we derive the first-order differential equations that describe the evolutions of radiation, baryon, CDM and dark energy densities in the universe. By analysing these equations, one can estimate the asymptotic evolution of the universe. To proceed, we start from the Friedmann equation

$$H^{2} + \frac{K}{a^{2}} = \frac{1}{3\bar{m}_{p}} \left( \rho_{r} + \rho_{b} + \rho_{c} + \rho_{d} \right), \tag{1}$$

where H is the Hubble parameter and the subscripts r, b, c and d correspond to the radiation, baryons, CDM and dark energy respectively. The parameter K denotes the curvature of the universe, where K=-1,0,+1 for the close, flat and open universe respectively. The above equation can be written in terms of the density parameters  $\Omega_K = K/(a^2H^2)$  and  $\Omega_{\alpha} = \rho_{\alpha}/(3\bar{m}_{\rm p}^2H^2)$  as

$$1 + \Omega_K = \sum_{\alpha = r, b, c, d} \Omega_{\alpha} = \Omega_r + \Omega_b + \Omega_c + \Omega_d.$$
 (2)

The index  $\alpha$  runs over the four species, namely radiation, baryons, CDM and dark energy. We now derive the autonomous equations for the dynamical variables  $\Omega_K$  and  $\Omega_{\alpha}$ . Differentiating  $\Omega_K = K/(a^2H^2)$  with respect to  $\ln a$ , we get

$$\Omega_K' = -\frac{2K}{H} \left( \frac{\dot{a}}{a^3 H^2} + \frac{\dot{H}}{a^2 H^3} \right) = -2\Omega_K \left( 1 + \frac{\dot{H}}{H^2} \right),\tag{3}$$

where the prime and dot denote the derivatives with respect to  $\ln a$  and time respectively. From the definition of the density parameter, one can show that

$$\Omega_{\alpha}' = \Omega_{\alpha} \left( \frac{\dot{\rho}_{\alpha}}{H \rho_{\alpha}} - 2 \frac{\dot{H}}{H^2} \right). \tag{4}$$

To study the evolution of the universe at late time, we will search for the fixed points of the above autonomous equations and check the stability of these fixed points. The fixed points of equations (3) and (4) are the points ( $\Omega_{Kc}$ ,  $\Omega_{\alpha c}$ ) at which

$$\Omega_K' = \Omega_\alpha' = 0. (5)$$

It follows from equation (3) that  $\Omega_K' = 0$  at  $\Omega_K = 0$  or  $1 + \dot{H}/H^2 = 0$ . Hence, possible fixed points at  $\Omega_K \neq 0$  correspond to the non-accelerating universe, i.e.  $1 + \dot{H}/H^2 \propto \ddot{a} = 0$ .

Since the expansion of the universe is accelerating today, we consider only the fixed points at  $\Omega_K = 0$ , and therefore neglect  $\Omega_K$  in our consideration for simplicity.

Now we come to the case of interacting holographic dark energy and use equation (4) to obtain the autonomous equation for this case. In the holographic dark energy scenario, the energy density of dark energy is related to the cosmological horizon L by

$$\rho_{\rm d} = 3c^2 \bar{m}_{\rm p}^2 L^{-2},\tag{6}$$

where c is a positive constant. Differentiating the above equation with respect to time, we obtain

$$\dot{\rho}_{\rm d} = -2\rho_{\rm d}\frac{\dot{L}}{L}.\tag{7}$$

We take the cosmological horizon to be the event horizon, which is defined as  $R_{\rm e}(t) = a(t) \int_t^{\infty} {\rm d}\tilde{t}/a(\tilde{t})$ . Hence,

$$\frac{\dot{L}}{L} = \frac{\dot{R}_{\rm e}}{R_{\rm e}} = H - \frac{1}{R_{\rm e}}.\tag{8}$$

We therefore get

$$\dot{\rho}_{\rm d} = -2H\rho_{\rm d} + 2\frac{\rho_{\rm d}^{3/2}}{\sqrt{3}c\bar{m}_{\rm p}}.$$
(9)

When dark energy has an interaction with CDM, the continuity equations yield

$$\dot{\rho}_{\rm c} = -3H\rho_{\rm c} + Q,\tag{10}$$

$$\dot{\rho}_{\rm d} = -3H(1+w_{\rm d})\rho_{\rm d} - Q,\tag{11}$$

where  $Q = 3H(\lambda_{\rm d}\rho_{\rm d} + \lambda_{\rm c}\rho_{\rm c})$ . Usually, one supposes that Q > 0 because the second law of thermodynamics might be violated if energy transfers from matter to dark energy (Q < 0). However, for generality, we will not restrict Q to be positive in our consideration. Comparing equation (9) with equation (11), we get

$$w_{\rm d} = -\frac{1}{3} - 2\frac{\sqrt{\Omega_{\rm d}}}{3c} - \frac{\lambda_{\rm d}\Omega_{\rm d} + \lambda_{\rm c}\Omega_{\rm c}}{\Omega_{\rm d}}.$$
 (12)

We assume that radiation and baryons have no interaction with dark energy, so that they obey the continuity equations

$$\dot{\rho}_{\rm r} = -4H\rho_{\rm r}$$
 and  $\dot{\rho}_{\rm b} = -3H\rho_{\rm b}$ . (13)

From equation (1), one can show that

$$2\frac{\dot{H}}{H^2} = \frac{(H^2)^{\cdot}}{H^3} = -3 + \Omega_{\rm d} + 2\frac{\Omega_{\rm d}^{3/2}}{c} + 3(\lambda_{\rm d}\Omega_{\rm d} + \lambda_{\rm c}\Omega_{\rm c}) - \Omega_{\rm r}.$$
 (14)

In the above equation, we set  $\Omega_K = 0$ . Using equations (4), (9), (13) and (14), we obtain

$$\Omega'_{\rm d} = \Omega_{\rm d} \left( 1 + 2 \frac{\Omega_{\rm d}^{1/2}}{c} - \Omega_{\rm d} - 2 \frac{\Omega_{\rm d}^{3/2}}{c} - 3(\lambda_{\rm d}\Omega_{\rm d} + \lambda_{\rm c}\Omega_{\rm c}) + \Omega_{\rm r} \right),$$
(15)

$$\Omega_{\rm c}' = \Omega_{\rm c} \left( \frac{3}{\Omega_{\rm c}} (\lambda_{\rm d} \Omega_{\rm d} + \lambda_{\rm c} \Omega_{\rm c}) - \Omega_{\rm d} - 2 \frac{\Omega_{\rm d}^{3/2}}{c} - 3(\lambda_{\rm d} \Omega_{\rm d} + \lambda_{\rm c} \Omega_{\rm c}) + \Omega_{\rm r} \right), \quad (16)$$

$$\Omega_{\rm r}' = \Omega_{\rm r} \left( -1 - \Omega_{\rm d} - 2 \frac{\Omega_{\rm d}^{3/2}}{c} - 3(\lambda_{\rm d}\Omega_{\rm d} + \lambda_{\rm c}\Omega_{\rm c}) + \Omega_{\rm r} \right),\tag{17}$$

$$\Omega_{\rm b}' = \Omega_{\rm b} \left( -\Omega_{\rm d} - 2 \frac{\Omega_{\rm d}^{3/2}}{c} - 3(\lambda_{\rm d}\Omega_{\rm d} + \lambda_{\rm c}\Omega_{\rm c}) + \Omega_{\rm r} \right). \tag{18}$$

The fixed points of the above equations are  $(\Omega_{\rm d}, \Omega_{\rm c}, \Omega_{\rm r}, \Omega_{\rm b}) = (0, 0, \Omega_{\rm rc}, 0)$ ,  $(0, 0, 0, \Omega_{\rm bc})$  and  $(\Omega_{\rm dc}, \Omega_{\rm cc}, 0, 0)$ . Since we are interested in the late time evolution of the universe, we will consider only the fixed point  $(\Omega_{\rm dc}, \Omega_{\rm cc}, 0, 0)$ . This fixed point can occur at late time, i.e., about the present or in the future, because  $\Omega_{\rm r}/\Omega_{\rm c}$  usually decreases with time and  $\Omega_{\rm b}/\Omega_{\rm c}$  can decrease with time if Q > 0. Using equations (15) and (16), the relation between  $\Omega_{\rm dc}$  and  $\Omega_{\rm cc}$  can be written as

$$1 + 2\frac{\Omega_{\rm dc}^{1/2}}{c} = \frac{3}{\Omega_{\rm cc}} (\lambda_{\rm d}\Omega_{\rm dc} + \lambda_{\rm c}\Omega_{\rm cc}). \tag{19}$$

From equation (2), we have  $\Omega_{\rm dc} + \Omega_{\rm cc} = 1$  and hence

$$1 - 3\lambda_{c} + 2\frac{\Omega_{dc}^{1/2}}{c} - (1 + 3\lambda_{d} - 3\lambda_{c})\Omega_{dc} - 2\frac{\Omega_{dc}^{3/2}}{c} = 0.$$
 (20)

The solution of equation (20) gives  $\Omega_{\rm dc}$  in terms of  $\lambda_{\rm d}$ ,  $\lambda_{\rm c}$  and c. Instead of finding the solution of this equation, we will use equation (19) to compute the cosmological parameters of interest in the following section. The basic idea is that there are various values of c,  $\lambda_{\rm d}$  and  $\lambda_{\rm c}$  that satisfy equation (19) for given  $\Omega_{\rm dc}$  and  $\Omega_{\rm cc}$ . Changes in the values of c,  $\lambda_{\rm d}$  and  $\lambda_{\rm c}$  lead to a different cosmological evolutions, i.e. a different  $w_{\rm d}$  for a given  $\Omega_{\rm dc}$  and  $\Omega_{\rm cc}$ .

The stability of this fixed point can be investigated by linearizing equations (15)–(18) around the fixed point and studying how the fluctuations around the fixed point evolve in time. If the amplitude of the fluctuations decreases in time, the fixed point is a stable fixed point or attractor. Linearizing equations (15)–(18) around ( $\Omega_{\rm dc}$ ,  $\Omega_{\rm cc}$ , 0, 0), we get

$$\delta\Omega_{\rm d}' = \left(\frac{\Omega_{\rm dc}^{1/2}}{c} - \Omega_{\rm dc} - 3\frac{\Omega_{\rm dc}^{3/2}}{c} - 3\lambda_{\rm d}\Omega_{\rm dc}\right)\delta\Omega_{\rm d} - 3\lambda_{\rm c}\Omega_{\rm dc}\delta\Omega_{\rm c} + \Omega_{\rm dc}\delta\Omega_{\rm r},\tag{21}$$

$$\delta\Omega_{\rm c}' = \left(-1 - 2\frac{\Omega_{\rm dc}^{1/2}}{c} + 3\lambda_{\rm c}\Omega_{\rm dc}\right)\delta\Omega_{\rm c} + \left(3\lambda_{\rm d} - \Omega_{\rm cc} - 3\Omega_{\rm cc}\frac{\Omega_{\rm dc}^{1/2}}{c} - 3\lambda_{\rm d}\Omega_{\rm cc}\right)\delta\Omega_{\rm d} + \Omega_{\rm cc}\delta\Omega_{\rm r},\tag{22}$$

$$\delta\Omega_{\rm r}' = -2\left(1 + \frac{\Omega_{\rm dc}^{1/2}}{c}\right)\delta\Omega_{\rm r},\tag{23}$$

$$\delta\Omega_{\rm b}' = -\left(1 + 2\frac{\Omega_{\rm dc}^{1/2}}{c}\right)\delta\Omega_{\rm b},\tag{24}$$

where  $\delta\Omega_{\alpha} = \Omega_{\alpha} - \Omega_{\alpha c}$  denote fluctuations around the fixed point. The above linear equations can be written as

$$\delta\Omega_{\alpha}' = M_{\alpha\beta}\delta\Omega_{\beta},\tag{25}$$

where  $\alpha$  and  $\beta$  run over the four species. The eigenvalues of the matrix M govern how the amplitude of the fluctuations around the fixed point changes with time. The fixed point is a stable, saddle or unstable point if all the eigenvalues are negative, some of the eigenvalues are positive or all the eigenvalues are positive, respectively (since we are dealing with real eigenvalues). The eigenvalues of the matrix M are

$$\lambda_{1} = \frac{\Omega_{\rm dc}^{1/2}}{c} - (1 + 3\lambda_{\rm d} - 3\lambda_{\rm c})\Omega_{\rm dc} - 3\frac{\Omega_{\rm dc}^{3/2}}{c},$$

$$\lambda_{2} = \lambda_{4} = -1 - 2\frac{\Omega_{\rm dc}^{1/2}}{c}, \qquad \lambda_{3} = -2\left(1 + \frac{\Omega_{\rm dc}^{1/2}}{c}\right).$$
(26)

Hence, the fixed point  $(\Omega_{\rm dc}, \Omega_{\rm cc}, 0, 0)$  is a stable point when  $\lambda_1 < 0$  and a saddle point when  $\lambda_1 > 0$ . Using equation (19),  $\lambda_1$  can be written as

$$\lambda_1 = \frac{3(\lambda_d \Omega_{dc} + \lambda_c \Omega_{cc})}{\Omega_{cc}} \left(\frac{1}{2} - \Omega_{dc}\right) - \frac{1}{2} - \frac{\Omega_{dc}^{3/2}}{c} - 3(\lambda_d - \lambda_c)\Omega_{dc}. \tag{27}$$

It is not easy to determine the sign of  $\lambda_1$  in general. Thus, we will determine it in particular cases in the next section.

#### 3. The attractor of cosmic evolution

We now consider the fixed point and stability of the cosmic evolution around the present epoch. For simplicity, we first consider the case where  $\lambda_{\rm d}=\lambda_{\rm c}=b^2$ . In this case, equation (19) becomes

$$1 + 2\frac{\Omega_{\rm dc}^{1/2}}{c} = \frac{3b^2}{\Omega_{cc}}. (28)$$

Since c > 0, equation (28) implies that  $b^2 \ge \Omega_{\rm cc}/3$ . This is the lower limit of  $b^2$  for the existence of the fixed point. From equations (12) and (28), it is easy to show that

$$w_{\rm d} = -\frac{b^2}{\Omega_{\rm cc}\Omega_{\rm dc}}. (29)$$

The equation of state parameter of the universe is defined as

$$w = \frac{p_{\text{total}}}{\rho_{\text{total}}} = \sum_{\alpha = \text{r,b,m,d}} w_{\alpha} \Omega_{\alpha}, \tag{30}$$

where  $w_{\alpha} = p_{\alpha}/\rho_{\alpha}$ . Since  $w_{\rm b} = w_{\rm c} = 0$  and  $\Omega_{\rm r}$  can be neglected at late time, we have  $w = w_{\rm d}\Omega_{\rm d}$  and therefore

$$w = -\frac{b^2}{\Omega_{cc}}. (31)$$

From the lower bound of  $b^2$ , we get  $w \leq 1/3$ . This means that the fixed point corresponds to cosmic acceleration. Moreover, one can see that the universe will be in the phantom phase, i.e., w < -1, if  $b^2 > \Omega_{\rm cc}$  or equivalently  $\Omega_{\rm dc}^{1/2} > c$ . Since the observations seem to indicate that  $w_{\rm d} < -1$  today, we find the value of  $b^2$  that makes  $w_{\rm d} < -1$  at the fixed point. It follows from equation (29) that  $w_{\rm d} < -1$  if  $b^2 > \Omega_{\rm cc}\Omega_{\rm dc}$ . We now check the stability of the fixed point. In this case, equation (27) becomes

$$\lambda_1 = \frac{3b^2}{\Omega_{cc}} \left( \frac{1}{2} - \Omega_{dc} \right) - \frac{1}{2} - \frac{\Omega_{dc}^{3/2}}{c}.$$
 (32)

It can be seen that it is not easy to find a point at which  $\lambda_1$  changes sign. However,  $\lambda_1$  is negative for any  $b^2$  or c if  $\Omega_{\rm dc} > 1/2$ , i.e.  $\Omega_{\rm dc} > \Omega_{\rm cc}$ . This means that the fixed point at which  $\Omega_{\rm dc} > \Omega_{\rm cc}$  is a stable fixed point or attractor, since the fixed point will occur when Q is positive and  $\Omega_{\rm r} = \Omega_{\rm b} = 0$ . At the present epoch  $\Omega_{\rm r}$  is small and can be neglected, and with positive Q the ratio  $\Omega_{\rm b}/\Omega_{\rm c}$  decreases with time, so the fixed point  $(\Omega_{\rm dc}, \Omega_{\rm cc}, 0, 0)$  will be reached in the future. From equations (15)–(18), one can see that if  $b^2$  is large,  $\Omega_{\rm b}$  can decrease quickly with time compared with  $\Omega_{\rm c}$ . As a result, the fixed point can be reached quickly near the present epoch. However, the CDM dominated epoch will disappear and the baryon fraction will be larger than the CDM fraction in the last scattering epoch due to the rapid decrease of  $\rho_{\rm b}/\rho_{\rm c}$  with time. This is excluded by the observed peak height ratio of the CMB power spectrum. Thus, on the basis of observations, the fixed point cannot be reached near the present for this case. We will see in the next section that small  $b^2$  or equivalently small  $\Omega_{\rm cc}$  is required by observations. Substituting  $\Omega_{\rm cc} = 1 - \Omega_{\rm dc}$  into equation (28), we get

$$1 - 3b^2 + 2\frac{\Omega_{dc}^{1/2}}{c} - \Omega_{dc} - 2\frac{\Omega_{dc}^{3/2}}{c} = 0.$$
 (33)

The above third-degree polynomial for  $\Omega_{\rm dc}^{1/2}$  will have one positive real root if  $1 > 3b^2$ . This root is the previously considered fixed point. In contrast, if  $1 \le 3b^2$  the above equation will have one additional real root. This root gives another fixed point at smaller  $\Omega_{\rm dc}$ . It is not hard to show that this fixed point is not stable and we will not consider it here.

Let us now consider the case where  $\lambda_d \neq \lambda_c$ . In this case, equation (19) becomes

$$1 + 2\frac{\Omega_{\rm dc}^{1/2}}{c} = \frac{3}{\Omega_{\rm cc}} \left( \lambda_{\rm d} \Omega_{\rm dc} + \lambda_{\rm c} \Omega_{\rm cc} \right). \tag{34}$$

Hence, the fixed point occurs when  $\lambda_d\Omega_{dc} + \lambda_c\Omega_{cc} > \Omega_{cc}/3$ . Using equations (12) and (34), we get

$$w_{\rm d} = -\frac{\lambda_{\rm d}\Omega_{\rm dc} + \lambda_{\rm c}\Omega_{\rm cc}}{\Omega_{\rm cc}\Omega_{\rm dc}},\tag{35}$$

and therefore

$$w = -\frac{\lambda_{\rm d}\Omega_{\rm dc} + \lambda_{\rm c}\Omega_{\rm cc}}{\Omega_{\rm cc}}.$$
 (36)

Like for the case when  $\lambda_{\rm d}=\lambda_{\rm c}$ , one can show that the fixed point occurs when  $w_{\rm d}<-1/(3\Omega_{\rm dc})$  or w<-1/3. Since the terms  $\lambda_{\rm d}\Omega_{\rm dc}$  and  $\lambda_{\rm c}\Omega_{\rm cc}$  from the interaction dominate at different times, the parameters  $\lambda_{\rm d}$  and  $\lambda_{\rm c}$  can be chosen such that the baryon fraction is smaller than the CDM fraction during the last scattering epoch although  $\Omega_{\rm cc}$  need not be very small. Thus, in this case, the attractor can be reached faster than for the case of  $\lambda_{\rm c}=\lambda_{\rm d}$ . From equation (27), we see that the fixed point is the stable fixed point when  $\Omega_{\rm dc}>\Omega_{\rm cc}$  and  $\lambda_{\rm c}$  is not much larger than  $\lambda_{\rm d}$ .

#### 4. The observational constraints

We now check the range of parameters for which the cosmic evolution has an attractor for compatibility with observations. We constrain the parameters of the interacting holographic dark energy using the latest observational data from SNIa [16] combined with the CMB shift parameter derived from three-year WMAP [17] and the baryon acoustic oscillations (BAO) from SDSS LRG [18].

The SNIa observations measure the apparent magnitude m of a supernova and its redshift z. The apparent magnitude m is related to the distance modulus  $\mu$  and luminosity distance  $d_L$  of the supernova by

$$\mu(z) = m(z) - M = 5 \log_{10}(d_L(z)/\text{Mpc}) + 25,$$
(37)

where M is the absolute magnitude of the supernova. For flat spacetime, the luminosity distance is given by

$$d_L(z) = H_0^{-1}(1+z) \int_0^z \frac{d\tilde{z}}{E(\tilde{z})}.$$
 (38)

Here,  $H_0$  is the present value of the Hubble parameter and  $E(z) = H(z)/H_0$ . To constrain the holographic dark energy model, we perform a  $\chi^2$  fit for the parameters  $\lambda_{\rm d}$ ,  $\lambda_{\rm c}$ , c,  $\Omega_{\rm c0}$ ,  $\Omega_{\rm b0}$ , where the subscript 0 denotes the present value. For  $\Omega_{\rm r0}$ , we compute its value from the CMB and neutrino temperatures. Using equation (2), one can compute  $\Omega_{\rm d0}$  from  $\Omega_{\rm c0}$ ,  $\Omega_{\rm b0}$  and  $\Omega_{\rm r0}$ . We have to include radiation in our consideration because it should not be neglected when we compute the CMB shift parameter. For the SNIa data, the parameter  $H_0$  is the nuisance parameter which needs to be marginalized out. Since the fit of holographic dark energy to SNIa data is sensitive to  $H_0$  [19], we have to add constraints from other observations to improve the fit. For this reason, we include the constraints from the CMB shift parameter and BAO measurements in our analysis.

The CMB shift parameter is a quantity derived from CMB data that has been shown to be model independent, so it can be used to constrain cosmological models. The CMB shift parameter is defined as [20]

$$R = \Omega_{\text{m0}}^{1/2} \int_0^{z_{\text{CMB}}} \frac{\mathrm{d}\tilde{z}}{E(\tilde{z})},\tag{39}$$

where  $\Omega_{\rm m0} = \Omega_{\rm c0} + \Omega_{\rm b0}$  and  $z_{\rm CMB} = 1089$  is the redshift at recombination. The estimated value of R from three-year WMAP data is  $1.70 \pm 0.03$ . From the SDSS data, the

measurement of the BAO peak in the distribution of SDSS LRG can be used to derive the model independent parameter A which is defined as [18]

$$A = \Omega_{\text{m0}}^{1/2} E(z_{\text{BAO}})^{-1/3} \left[ \frac{1}{z_{\text{BAO}}} \int_{0}^{z_{\text{BAO}}} \frac{d\tilde{z}}{E(\tilde{z})} \right]^{2/3}, \tag{40}$$

where  $z_{\text{BAO}} = 0.35$ . The estimated A is  $A = 0.469(n_{\text{s}}/0.98)^{-0.35} \pm 0.017$ . According to the three-year WMAP data, the scalar spectral index is chosen to be  $n_{\text{s}} = 0.95$ .

We first consider the case where  $\lambda_{\rm d}=\lambda_{\rm c}=b^2$ . For simplicity, we start by neglecting baryons in our consideration. Hence the attractor becomes  $(\Omega_{\rm d},\Omega_{\rm c},\Omega_{\rm r})=(\Omega_{\rm dc},\Omega_{\rm cc},0)$ , where  $\Omega_{\rm dc}$  and  $\Omega_{\rm cc}$  satisfy equation (28). The region of  $b^2$  and  $\Omega_{\rm cc}$  for which the fixed point exists and the 99.7% confidence regions from the combined constraints are shown in figure 1. From this figure, one sees that a small  $b^2$  is required by observations, so that the attractor that satisfies the observational constraints occurs at low  $\Omega_{\rm cc}$ . This implies that the attractor cannot occur at present, where  $\Omega_{\rm c}\approx 0.3$ . In the future,  $\Omega_{\rm c}$  can become small, so the fixed point can exist. Nevertheless, if the attractor is reached in the far future, the cosmic coincidence may not be alleviated because the present values of  $\Omega_{\rm c}$  and  $w_{\rm d}$  may not satisfy the observational constraints. In the following consideration, we will study how the ratio r evolves during the present epoch to check the possibility of alleviating the cosmic coincidence. Since the physical fixed point cannot occur if  $b^2 < 0$ , we perform another fit by supposing that  $b^2 \geq 0$ . The result is shown in figure 1. It can be seen that the above conclusions for the case of arbitrary  $b^2$  are also valid for the case of  $b^2 \geq 0$ .

The situation changes a bit when we include baryons in our consideration. From the previous section, we know that the cosmic evolution reaches the attractor at  $(\Omega_{\rm d}, \Omega_{\rm c}, \Omega_{\rm b}, \Omega_{\rm r}) = (\Omega_{\rm dc}, \Omega_{\rm cc}, 0, 0)$ . Since the present value of  $\Omega_{\rm b}$  does not vanish, this attractor cannot occur at present. However, the attractor can occur in the future because the ratio  $\Omega_{\rm b}/\Omega_{\rm c}$  decreases with time due to the positive Q. It can be seen that the ratio  $\Omega_{\rm b}/\Omega_{\rm c}$  decreases faster when  $b^2$  increases. According to the observational constraints, a small  $b^2$  is also required in this case, so that the attractor is slowly reached in the future. In order to perform a fit for this case, we use a prior  $\Omega_{\rm b0} = 0.047 \pm 0.006$  from the one-year WMAP data [21] because  $\Omega_{\rm b0}$  cannot be constrained very well by using only SNIa data, the CMB shift parameter and BAO measurements. It can be seen from figure 1 that the shape of the confidence contours does not change much when we include non-interacting baryons in our consideration. Obviously, the contours move to the left when the amount of  $\Omega_{\rm b0}$  increases. This is because the amount of  $\Omega_{\rm c0}$  decreases.

We now consider the case of arbitrary  $\lambda_{\rm d}$  and  $\lambda_{\rm c}$ . We also perform a  $\chi^2$  fit for the case with baryons and without baryons. For the case where baryons are neglected, it follows from figure 2 that the attractor can occur at present ( $\Omega_{\rm cc}\approx 0.3$ ) for a narrow range of  $\lambda_{\rm d}$  and  $\lambda_{\rm c}$ . Nevertheless, a small  $\Omega_{\rm cc}$  is required by observations if we restrict  $\lambda_{\rm d}$  and  $\lambda_{\rm c}$  to being positive. This implies that the attractor must occur in the future. Similarly to the case for  $\lambda_{\rm d}=\lambda_{\rm c}=b^2$ , the attractor cannot be reached at present if baryons are included in the consideration. Nevertheless, for suitable values of  $\lambda_{\rm c}$  and  $\lambda_{\rm d}$  which satisfy the observational constraints, the attractor in this case can be reached faster than for the case of  $\lambda_{\rm c}=\lambda_{\rm d}$ .

In order to check whether the cosmic coincidence can be alleviated for this form of interaction, we study the evolution of r during the present epoch. Since the evolutions

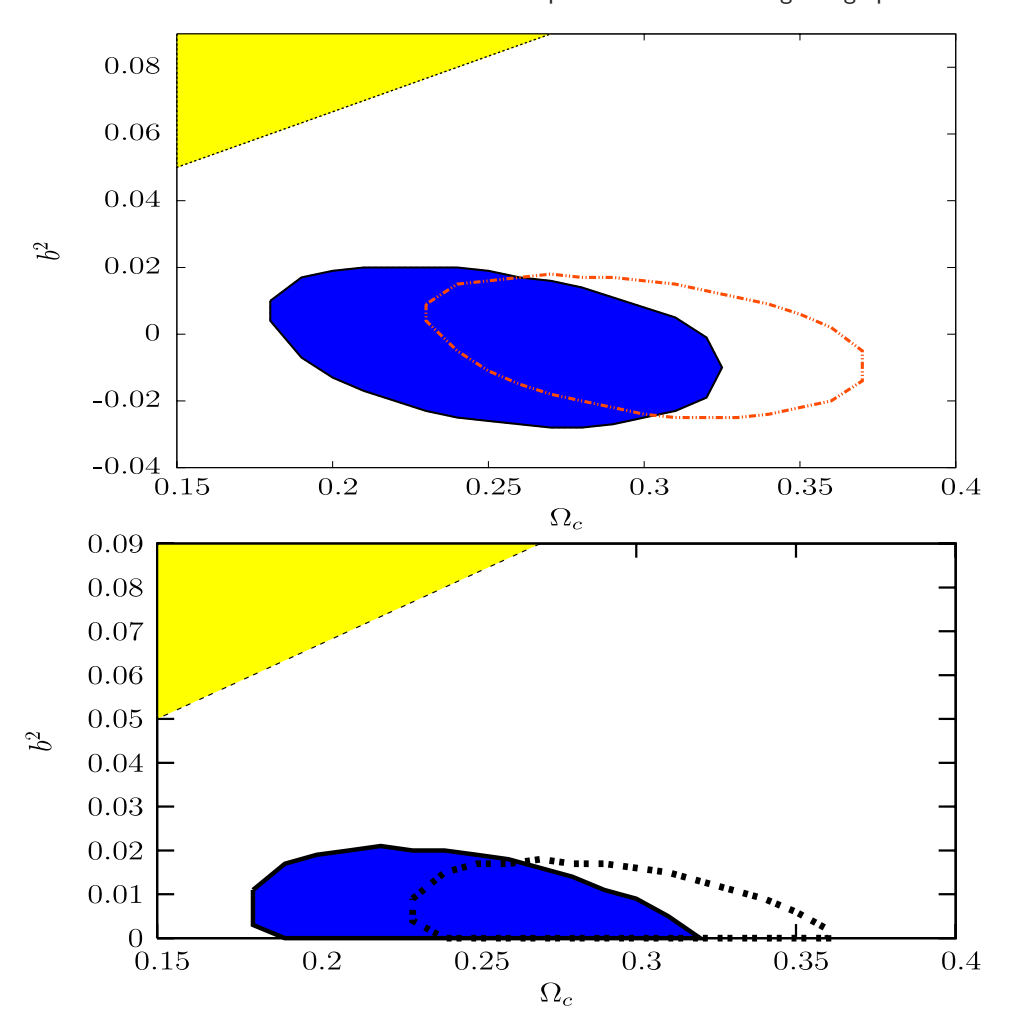


Figure 1. A region of parameters  $b^2$  and  $\Omega_c$  in which the cosmic evolution has a late time attractor (the yellow regions above the dashed lines), and the 99.7% confidence levels from the combined analysis of SNIa data, the CMB shift parameter and BAO measurements. For the yellow region,  $\Omega_c$  refers to  $\Omega_{cc}$ , but  $\Omega_c$  refers to  $\Omega_{c0}$  for the confidence levels. The upper panel shows the case of arbitrary  $b^2$ , while the lower panel shows the case where  $b^2 \geq 0$ . The blue regions represent the confidence regions for the case that includes baryons and prior  $\Omega_{b0} = 0.047 \pm 0.006$ , while the thick dotted lines represent the confidence levels for the case where baryons are neglected.

of r for the cases with baryons and without baryons have nearly the same features, we consider only the latter case. We first consider the case where  $b^2 = \lambda_{\rm c} = \lambda_{\rm d}$ . Setting  $b^2$ , c and  $\Omega_{\rm c0}$  equal to their best fit values, i.e.  $b^2 = -0.004$ , c = 0.84 and  $\Omega_{\rm c0} = 0.3$ , the evolutions of r and  $r' = \dot{r}/(rH)$  are plotted in figure 3. From figure 3, we see that |r'| > 1 during the present epoch because  $\Omega_{\rm c0}$  is quite different from  $\Omega_{\rm cc}$ . Due to a negative  $b^2$ , r and  $\Omega_{\rm c}$  become negative and consequently reach the attractor at late time. Recall that  $\Omega_{\rm c} > 0$  at the attractor if  $b^2 \ge \Omega_{\rm cc}/3$ . To solve the coincidence problem, the ratio r should vary slowly during the present epoch such that  $|r'| \lesssim 1$  today [4]. The present value of |r'| will decrease if the value of  $\Omega_{\rm cc}$  gets closer to the value of  $\Omega_{\rm c0}$ , i.e. the cosmic evolution

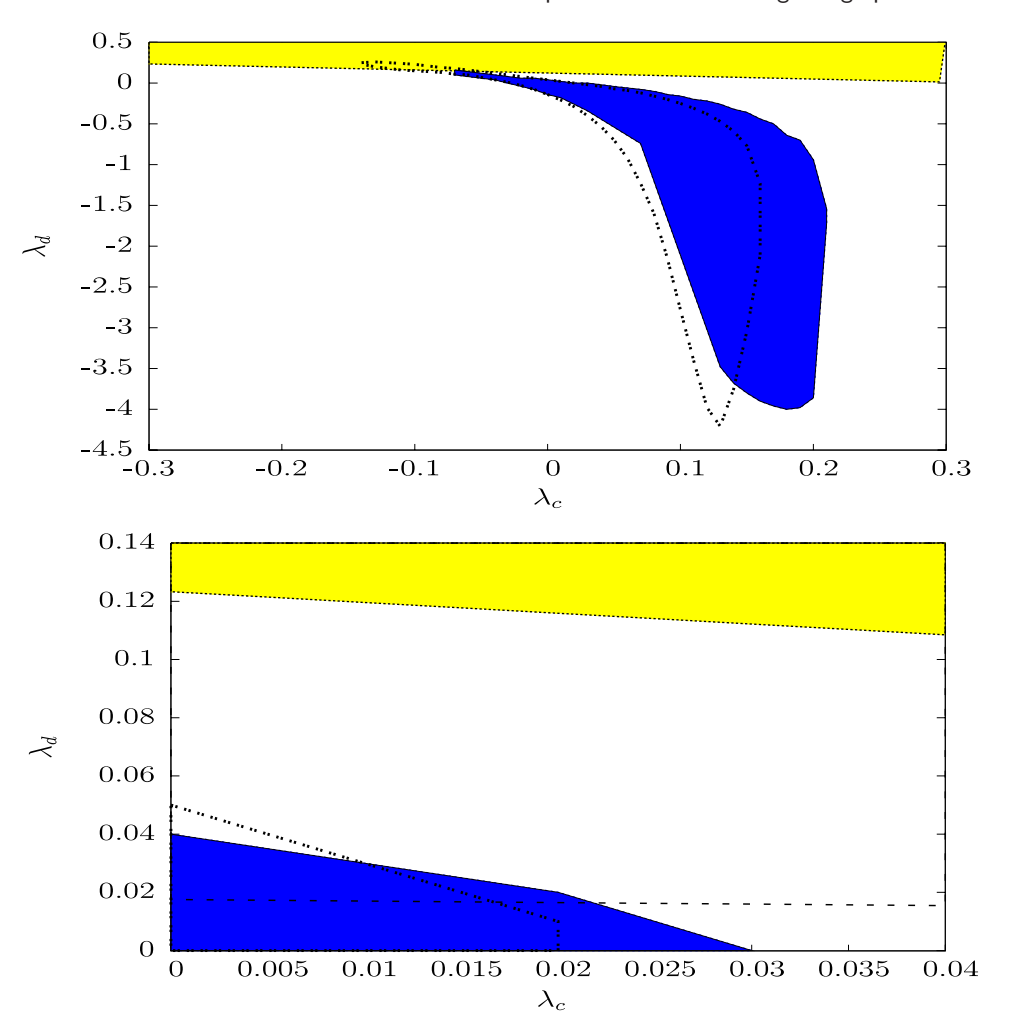


Figure 2. A region of parameters  $\lambda_{\rm d}$  and  $\lambda_{\rm c}$  for which the cosmic evolution has a late time attractor (the yellow regions above the dashed lines), and the 99.7% confidence levels from the combined analysis of SNIa data, the CMB shift parameter and BAO measurements. The upper panel shows the case for arbitrary  $\lambda_{\rm d}$  and  $\lambda_{\rm c}$ , while the lower panel shows the case where  $\lambda_{\rm d}, \lambda_{\rm c} \geq 0$ . The blue regions represent the confidence regions for the case that includes baryons and prior  $\Omega_{\rm b0} = 0.047 \pm 0.006$ , while the thick dotted lines represent the confidence levels for the case where baryons are neglected. The dashed lines are plotted by setting  $\Omega_{\rm cc} = 0.27$ , but the thick dashed line in the lower panel is plotted by setting  $\Omega_{\rm cc} = 0.05$ . We note that the region above the thick dashed line also represents the region for which the cosmic evolution has an attractor.

reaches the attractor near the present. According to the yellow region in figure 1, the value of  $\Omega_{\rm cc}$  will increase and get closer to  $\Omega_{\rm c0}$  if  $b^2$  increases. However, |r'| during the present epoch will be smaller than 1 only when  $b^2$  is larger than the observational bound. The evolution of r for the case where  $\Omega_{\rm cc}$  is close to  $\Omega_{\rm c0}$  is shown in figure 3. In this case, the values of c and  $\Omega_{\rm c0}$  are the best fit values, while the value of  $b^2$  is larger than the observational bound but is inside the yellow region in figure 1. From figure 3 we see that |r'| < 1 during the present epoch in this case but the amount of  $\Omega_{\rm c}$  during the early

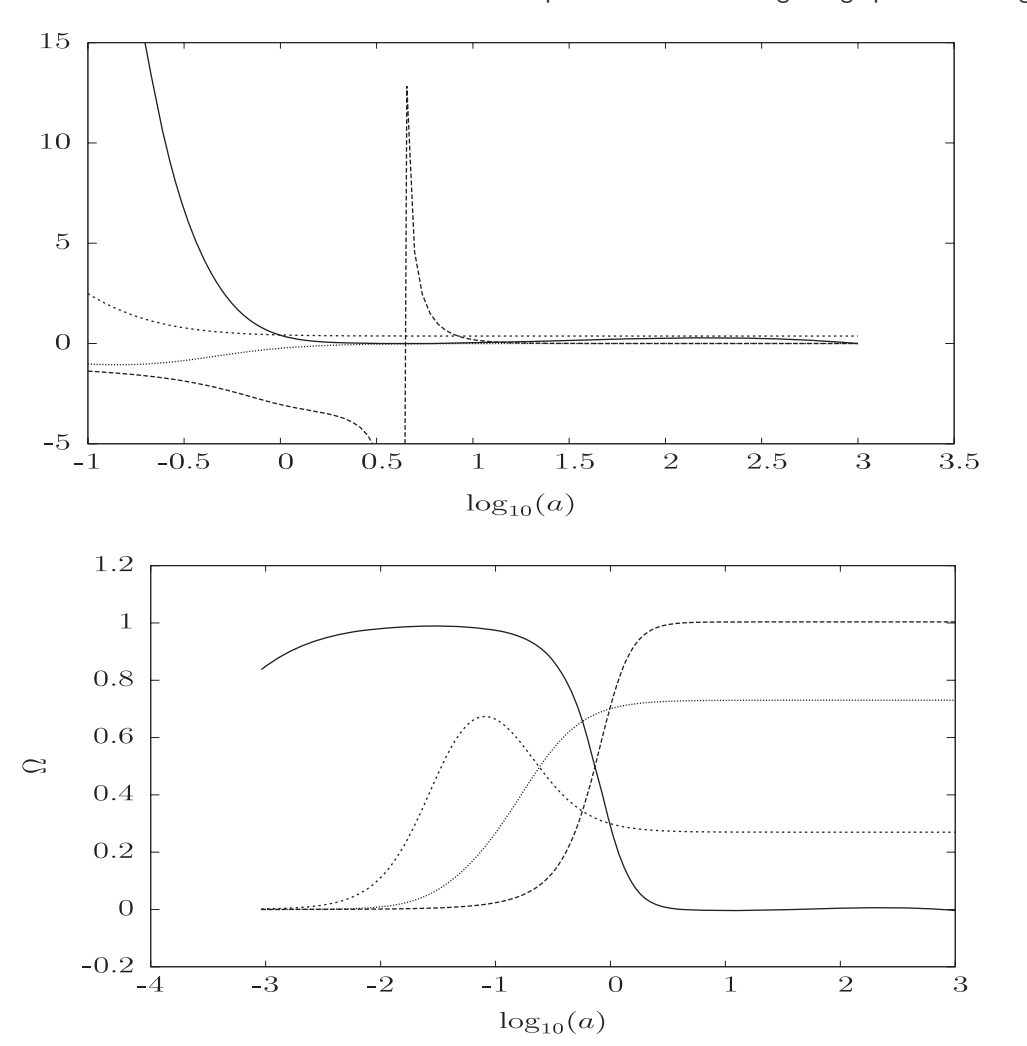


Figure 3. The upper panel shows the evolutions of r (solid and dashed lines) and  $\dot{r}/(rH)$  (long dashed and dotted lines), while the lower panel shows the evolutions of  $\Omega_{\rm c}$  (solid and dashed lines) and  $\Omega_{\rm d}$  (long dashed and dotted lines). The solid and long dashed lines correspond to the case where the values of  $b^2$ , c and  $\Omega_{\rm c0}$  are equal to their best fit values, while the dashed and dotted lines correspond to the case where  $b^2$  is chosen such that  $\Omega_{\rm cc}$  is close to  $\Omega_{\rm c0}$ , i.e.  $\Omega_{\rm cc} = 0.27$ .

time is too small. For this reason, this case does not satisfy the observational constraints. Hence, in the case of  $\lambda_c = \lambda_d$ , the coincidence problem is not really alleviated for this form of interaction terms.

Next, we consider the case where  $\lambda_{\rm c} \neq \lambda_{\rm d}$ . We first set c,  $\lambda_{\rm c}$ ,  $\lambda_{\rm d}$  and  $\Omega_{\rm c0}$  equal to their best fit values, i.e. c=0.37,  $\lambda_{\rm c}=0.08$ ,  $\lambda_{\rm d}=-0.45$  and  $\Omega_{\rm c0}=0.27$ . This choice of the parameter value is outside the yellow region in figure 2. Since the interaction term Q is dominated by  $3H\lambda_{\rm d}\Omega_{\rm d}$  during the present epoch, Q becomes negative at present. Hence, r and also  $\Omega_{\rm c}$  become negative and consequently reach the attractor at late time. Of course, the attractor in this case does not correspond to the physical attractor. The evolutions of r and  $\Omega_{\rm c}$  are shown in figure 4. Similarly to the case for  $\lambda_{\rm c}=\lambda_{\rm d}$ , the present value of |r'| for this choice of parameter values is larger than 1 because  $\Omega_{\rm cc}$  is quite different from  $\Omega_{\rm c0}$ .

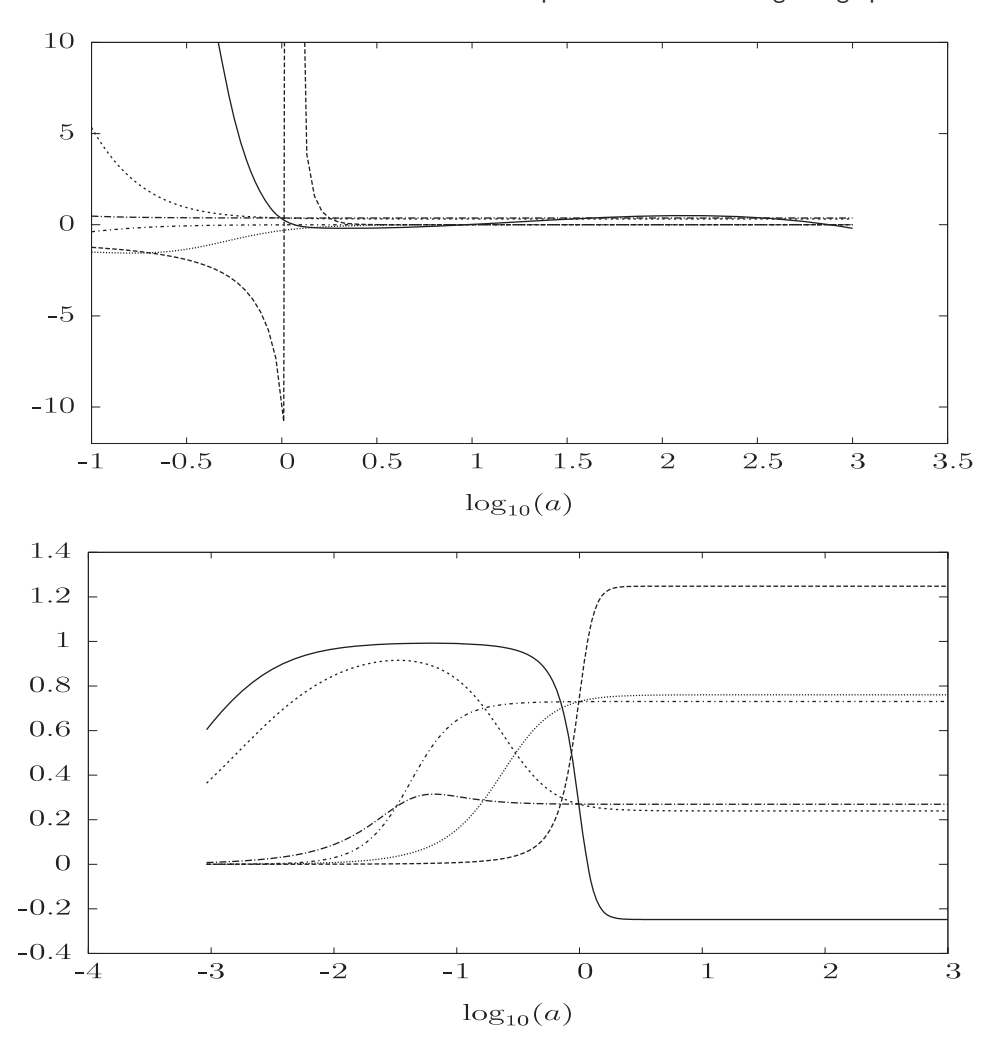


Figure 4. The upper panel shows the evolutions of r (solid, dashed and long dashed–dotted lines) and  $\dot{r}/(rH)$  (long dashed, dotted and dashed–dotted lines), while the lower panel shows the evolutions of  $\Omega_{\rm c}$  (solid, dashed and long dashed–dotted lines) and  $\Omega_{\rm d}$  (long dashed, dotted and dashed–dotted lines). The solid and long dashed lines correspond to the case where the values of  $\lambda_{\rm c}$ ,  $\lambda_{\rm d}$ , c and  $\Omega_{\rm c0}$  are equal to their best fit values, the dashed and dotted lines correspond to the case where c,  $\lambda_{\rm c}$  and  $\lambda_{\rm d}$  are chosen such that  $\Omega_{\rm cc}$  is close to  $\Omega_{\rm c0}$ , i.e.  $\Omega_{\rm cc}=0.24$ , and the long dashed–dotted and dashed–dotted lines correspond to the case where c,  $\lambda_{\rm c}$  and  $\lambda_{\rm d}$  are chosen such that  $\Omega_{\rm cc}=\Omega_{\rm c0}$ .

We now keep  $\Omega_{\rm c0}$  fixed and choose the new values of parameters c,  $\lambda_{\rm c}$  and  $\lambda_{\rm d}$  such that the observational constraints are satisfied and the cosmic attractor occurs at  $\Omega_{\rm cc}=0.24$  near the present epoch. This choice of the parameter values is inside the intersection between the yellow region and the confidence region in figure 2. From figure 4, we see that the present value of |r'| is smaller than 1 and the attractor is reached near the present epoch for this choice of the parameter values. On the basis of the soft coincidence idea, the coincidence problem can be alleviated in this case. The coincidence problem is better alleviated if  $\Omega_{\rm cc}=\Omega_{\rm c0}$  or equivalently if the cosmic attractor is reached at the present.

Unfortunately, the parameter values that make  $\Omega_{\rm cc} = \Omega_{\rm c0}$  do not satisfy the observational constraints. The evolutions of r and  $\Omega_{\rm c}$  for this case are shown in figure 4. From the figure, it is clear that this case is ruled out by observations. We note that the present value of |r'| will increase if we include baryons in the above consideration.

Finally, we estimate whether |r'| can be smaller than 1 at present if we constrain the parameters of dark energy using the SDSS matter power spectrum. Here, we will not perform a complete fit for this data set because the nature of the perturbations in holographic dark energy is not yet completely understood. To write down the evolution equations for the density perturbation and compute the matter power spectrum for this interacting dark energy model, we use the assumption below. From the results in [22], we suppose that the perturbation in holographic dark energy can be neglected when  $kR_{\rm e}/a\gg 1$ , where k is the wavenumber of the perturbation modes. Using equations (1) and (6) and supposing that radiation can be neglected during matter domination, one can show that  $H^{-1}/R_{\rm e}=\sqrt{\Omega_{\rm d}}/c$ , i.e. the Hubble radius is smaller than the event horizon if  $\sqrt{\Omega_{\rm d}}< c$ . Since we use the data from SDSS which measures the matter power spectrum on scales smaller than the Hubble radius, we neglect the perturbation in holographic dark energy in the calculation of the matter power spectrum. We write the perturbed interaction term using the formulae in [23, 24], so that the evolution equations for the perturbation in CDM are

$$\frac{\mathrm{d}\Delta_{\mathrm{c}}}{\mathrm{d}\eta} = -kV_{\mathrm{c}} + 3\mathcal{H}\Psi\left(\lambda_{\mathrm{c}} + \lambda_{\mathrm{d}}\frac{\rho_{\mathrm{d}}}{\rho_{\mathrm{c}}}\right) - 3\frac{\mathrm{d}\Phi}{\mathrm{d}\eta}\left(\lambda_{\mathrm{c}} + \lambda_{\mathrm{d}}\frac{\rho_{\mathrm{d}}}{\rho_{\mathrm{c}}}\right) - 3\mathcal{H}\lambda_{\mathrm{d}}\Delta_{\mathrm{c}}\frac{\rho_{\mathrm{d}}}{\rho_{\mathrm{c}}},$$

$$\frac{\mathrm{d}V_{\mathrm{c}}}{\mathrm{d}\eta} = -\mathcal{H}V_{\mathrm{c}} + k\Psi,$$
(41)

where  $\Delta_{\rm c}$  and  $V_{\rm c}$  are the gauge-invariant density contrast and velocity perturbation of CDM,  $\Psi$  and  $\Phi$  are the metric perturbations,  $\mathcal{H} = a^{-1}(da/d\eta)$  and  $\eta$  is the conformal time. We solve the above equations, compute the matter power spectrum and compare the matter power spectrum obtained with SDSS data using CMBEASY [25]. By checking the value of  $\chi^2$ , we have found that the best fit parameters for this data set are different from the best fit parameters from the observational constraints on the homogeneous universe. Instead of searching for the best fit parameters for this data set, we roughly check the viability of the parameters by comparing the matter power spectrum of the models considered with the matter power spectrum for the  $\Lambda$ CDM model whose parameters are taken from the best fit value for three-year WMAP and SDSS data [26]. In figure 5, we plot the fractional difference in matter power spectrum between the interacting holographic dark energy and  $\Lambda$ CDM models. From this figure, we see that for suitable ranges of dark energy parameters, |r'| can be smaller than 1 at present and the difference in matter power spectrum can be smaller than the error for the matter power spectrum of SDSS data. This implies that the alleviation of the coincidence problem by this interacting dark energy model is not excluded by SDSS data.

#### 5. Conclusions

For the interacting holographic dark energy model, we study the fixed points and their stability, and compare a range of model parameters for which an attractor exists with the 99.7% confidence levels from the combined analysis of SNIa data, the CMB shift

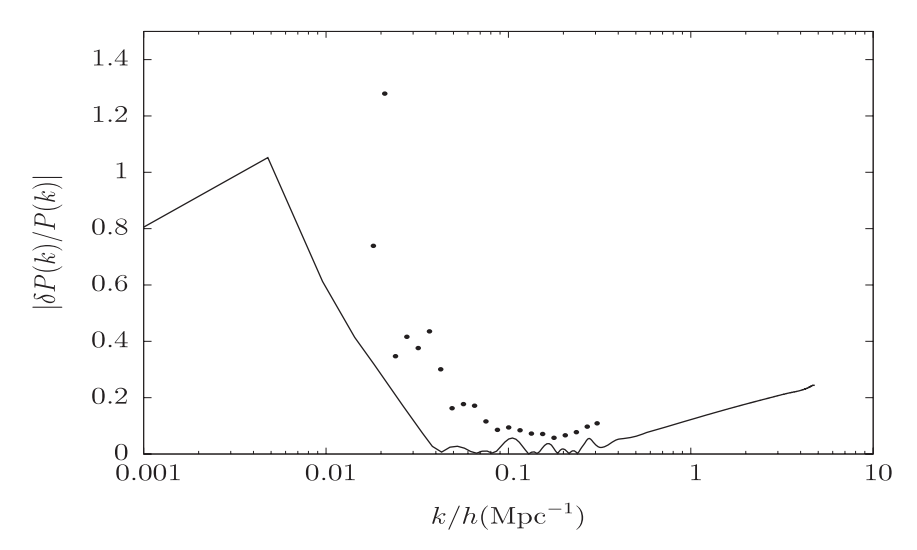


**Figure 5.** The fractional difference in matter power spectrum  $|\delta P(k)/P(k)|$  between the interacting holographic dark energy and  $\Lambda \text{CDM}$  models. For this plot, the parameters of dark energy are chosen such that  $|r'| \approx 0.9$  at present. The fractional error for the matter power spectrum  $|\delta P(k)/P(k)| = \text{error/spectrum}$  of SDSS data is represented by dots.

parameter and BAO measurements. Neglecting baryons, the observational constraints require that the value of  $\Omega_c$  at the attractor point must be small if  $\lambda_d = \lambda_c$  or  $\lambda_d, \lambda_c > 0$ . This implies that the cosmic evolution will reach the attractor point in the future when  $\Omega_{\rm c}$  becomes small. In this case, r cannot be slowly varying during the present epoch and the cosmic attractor cannot be reached near the present. Hence, the coincidence problem is not really alleviated for this case. However, if  $\lambda_{\rm d}$  and  $\lambda_{\rm c}$  are allowed to be negative, the cosmic evolution can reach the attractor near the present epoch for a narrow range of  $\lambda_{\rm d}$ and  $\lambda_c$ . Therefore, it is possible to alleviate the coincidence problem in this case. Including baryons in our consideration, the attractor of the cosmic evolution cannot occur at present due to the non-vanishing baryon fraction. According to observations, the fixed point in this case is possible only when Q is small and positive. Hence, the fixed point will be slowly reached in the future. These results indicate that for the interacting holographic dark energy model with the interaction terms considered here, the cosmic coincidence problem cannot be alleviated very well. We also briefly considered the constraint from the SDSS matter power spectrum on the dark energy parameters. We have found that the parameters ranges that lead to the alleviation of the cosmic coincidence are allowed by SDSS data.

#### **Acknowledgments**

The author would like to thank Bin Wang for helpful discussions and suggestions and for hospitality at Fudan University during the final stage of this work. He also thanks A Ungkitchanukit and an anonymous referee for comments on the manuscript. The observational fitting was performed using the workstation of the Biophysics group, Kasetsart University. This work is supported by Thailand Research Fund (TRF) and vcharkarn.com.

#### References

- [1] Riess A G et al, Observational evidence from supernovae for an accelerating universe and a cosmological constant, 1998 Astron. J. 116 1009 [SPIRES] [astro-ph/9805201]
- [2] Perlmutter S et al, Measurements of Omega and Lambda from 42 high-redshift supernovae, 1999 Astrophys.
   J. 517 565 [SPIRES] [astro-ph/9812133]
- [3] Zimdahl W and Pavón D, Scaling cosmology, 2003 Gen. Rel. Grav. 35 413 [SPIRES] [astro-ph/0210484]
- [4] del Campo S, Herrera R, Olivares G and Pavón D, Interacting models of soft coincidence, 2006 Phys. Rev. D 74 023501 [SPIRES] [astro-ph/0606520]
- [5] Sadjadi H M and Alimohammadi M, Cosmological coincidence problem in interacting dark energy models, 2006 Phys. Rev. D 74 103007 [SPIRES] [gr-qc/0610080]
- [6] Amendola L, Coupled quintessence, 2000 Phys. Rev. D 62 043511 [SPIRES] [astro-ph/9908023]
- [7] Chimento L P, Jakubi A S, Pavón D and Zimdahl W, Interacting quintessence solution to the coincidence problem, 2003 Phys. Rev. D 67 083513 [SPIRES] [astro-ph/0303145]
- [8] Cohen A G, Kaplan D B and Nelson A E, Effective field theory, black holes, and the cosmological constant, 1999 Phys. Rev. Lett. 82 4971 [SPIRES] [hep-th/9803132]
- [9] Li M, A model of holographic dark energy, 2004 Phys. Lett. B 603 1 [SPIRES] [hep-th/0403127]
- [10] Setare M R and Vagenas E C, The cosmological dynamics of interacting holographic dark energy model, 2007 Preprint 0704.2070
- [11] Setare M R, Interacting holographic dark energy model in non-flat universe, 2006 Phys. Lett. B 642 1 [SPIRES] [hep-th/0609069]
- [12] Setare M R, Bulk-brane interaction and holographic dark energy, 2006 Phys. Lett. B 642 421 [SPIRES] [hep-th/0609104]
- [13] Setare M R, Interacting holographic phantom, 2007 Eur. Phys. J. C 50 991 [hep-th/0701085]
- [14] Elizalde E, Nojiri S, Odintsov S D and Wang P, Dark energy: vacuum fluctuations, the effective phantom phase, and holography, 2005 Phys. Rev. D 71 103504 [SPIRES] [hep-th/0502082]
- [15] Gong Y, Wang B and Wang A, Thermodynamical properties of dark energy, 2007 Phys. Rev. D 75 123516 [SPIRES] [gr-qc/0611155]
- [16] Riess A G et al, New Hubble Space Telescope discoveries of type Ia supernovae at z > 1: narrowing constraints on the early behavior of dark energy, 2006 Preprint astro-ph/0611572
- [17] Wang Y and Mukherjee P, Observational constraints on dark energy and cosmic curvature, 2006 Astrophys. J. 650 1 [SPIRES] [astro-ph/0703780]
- [18] Eisenstein D J et al, Detection of the baryon acoustic peak in the large-scale correlation function of SDSS luminous red galaxies, 2005 Astrophys. J. 633 560 [SPIRES] [astro-ph/0501171]
- [19] Zhang X and Wu F, Constraints on holographic dark energy from type Ia supernova observations, 2005 Phys. Rev. D 72 043524 [SPIRES] [astro-ph/0506310]
- [20] Zhang X and Wu F, Constraints on holographic dark energy from latest supernovae, galaxy clustering, and cosmic microwave background anisotropy observations, 2007 Phys. Rev. D 76 023502 [SPIRES] [astro-ph/0701405]
- [21] Spergel D N et al, First year Wilkinson Microwave Anisotropy Probe (WMAP) observations: determination of cosmological parameters, 2003 Astrophys. J. Suppl. 148 175 [astro-ph/0302209]
- [22] Li M, Lin C and Wang Y, Some issues concerning holographic dark energy, 2008 Preprint 0801.1407
- [23] Kodama H and Sasaki M, Cosmological perturbation theory, 1984 Prog. Theor. Phys. Suppl. 78 1
- [24] Malik K, Cosmological perturbations in an inflationary universe, 2001 Preprint astro-ph/0101563
- [25] Doran M, Cmbeasy:: an object oriented code for the cosmic microwave background, 2005 J. Cosmol. Astropart. Phys. JCAP10(2005)011 [SPIRES] [astro-ph/0302138]
- [26] Spergel D N et al, Wilkinson Microwave Anisotropy Probe (WMAP) three year results: implications for cosmology, 2007 Astrophys. J. Suppl. 170 377 [astro-ph/0603449]

## CMB constraints on spacetime noncommutativity in inflationary scenario

#### Khamphee Karwan

Theoretical High-Energy Physics and Cosmology Group, Department of Physics, Chulalongkorn University, Bangkok 10330, Thailand Present address: Department of Physics, Faculty of Science, Kasetsart University, Bangkok 10900, Thailand

#### Abstract.

We investigate the primordial power spectrum of the density perturbations based on the assumption that spacetime is noncommutative in the early stage of inflation, and constrain the contribution from spacetime noncommutativity on the CMB anisotropies. Due to the spacetime noncommutativity, the primordial power spectrum can lose rotational invariance. Using the power law k-inflation model, we show that the deviation from rotational invariance of the primordial power spectrum depends on the ratio  $L_s^4/c_s^2$ , where  $L_s$  is the noncommutative length scale and  $c_s$  is the sound speed of inflaton. We compute the covariance matrix for the harmonic coefficients of the CMB anisotropies from this direction-dependent primordial power spectrum, and constrain the contributions from the spacetime noncommutativity on this covariance matrix using five-year WMAP CMB maps. We find that the upper boundthe for the ratio  $L_s c_s^{1/(\beta-1)}/\beta^{1/2}$  is  $1.4 \times 10^{-28}$ cm at 99.7% confidence level. Taking the values of  $c_s$  and  $\beta$  to be known precisely, and with  $\beta$  being the inverse of the slow-roll parameter, the upper bound for  $L_s$  is estimated to be less than  $10^{-27}$ cm at 99.7% confidence level.

**Keywords**: inflation.

#### 1. Introduction

The inflationary cosmology [1, 2, 3] is the scenario of the very early universe. It provides a successful mechanism for generating nearly scale invariant primordial density perturbations, that give rise to galaxy formation and temperature anisotropies in the CMB which are in agreement with observation [4]. If the period of inflation is sufficiently longer than that required for solving the horizon and flatness problems, such that the wavelengths of perturbations which are observed today emerged from the Planck regime in the early stages of inflation, the physics on trans-Planckian scales should leave an imprint on the primordial density perturbations [5, 6]. Here, we consider the imprint of trans-Planckian physics based on noncommutative spacetime.

Near the Planck scale, the properties of spacetime are expected to be modified due to the quantum nature of gravity [7]. It has been shown that a consequence of string theory which is a promising candidate of quantum gravity, is that the spacetime is noncommutative [8]

$$[x^{\mu}, x^{\nu}] = i\Theta^{\mu\nu}(x),\tag{1}$$

where  $\Theta^{\mu\nu}$  is an antisymmetric tensor.

The influences of spacetime noncommutativity on the feature of power spectrum of primordial fluctuations have been studied by many authors [9] - [16]. For the case where  $\Theta^{ij} = 0$  but  $\Theta^{0i} \neq 0$  [9, 10, 11], the contribution from spacetime noncommutativity can lead to the running of the spectral index of the primordial power spectrum. For the case where  $\Theta^{ij} \neq 0$  but  $\Theta^{0i} = 0$  [12, 13], the primordial power spectrum can become directiondependent, and consequently the statistics of CMB fluctuations becomes anisotropic. We are interested in this spacetime noncommutativity induced statistical anisotropy. @@ Usually, the statistics of the CMB temperature fluctuations is supposed to be isotropic. Hence, if the non-Gaussianity of the CMB fluctuations is assumed to be negligible, the statistical properties of the CMB fluctuations will be completely described by the angular power spectrum [17]. However, recently there are many attempts to check whether the statistics of the CMB fluctuations is perfectly isotropic by searching for the statistical anisotropy contributions in the CMB sky maps [18, 19, 20]. In the case where the statistics of the CMB fluctuations is anisotropic, the angular power spectrum does not contain all the information about the statistical properties of the CMB fluctuations even when the Gaussianity of the CMB fluctuations is assumed. Some of the estimators for quantifying the statistical anisotropy contributions in the CMB fluctuations have been proposed in [21, 17, 22]. According to [18, 19], the statistics of the observed CMB fluctuations does not deviate from isotropy significantly.

In this work, we constrain the contributions from spacetime noncommutativity on CMB temperature fluctuations using five-year WMAP CMB maps. In the next section, we compute the primordial power spectrum of the power law k-inflation by taking the spacetime noncommutativity of the form  $\Theta^{ij} \neq 0$  and  $\Theta^{0i} = 0$ . In section 3, we compute the covariance matrix for the harmonic coefficients of the CMB temperature fluctuations

 $\langle a_{lm}^* a_{l'm'} \rangle$ , and constrain the contributions from spacetime noncommutativity using CMB maps. Finally, we conclude in section 4.

#### 2. The contributions from spacetime noncommutativity

We now investigate the contributions from spacetime noncommutativity on the primordial power spectrum of the k-inflaton whose action is givven by [23]

$$S = \int d^4x \sqrt{-g} \left[ \frac{\bar{m}_p^2 R}{2} + P(X, \phi) \right], \tag{2}$$

where  $\bar{m}_p = (8\pi G)^{-1/2}$  is the reduced Planck mass,  $\phi$  is the inflaton field and  $X = (1/2)g^{\mu\nu}\partial_{\mu}\phi\partial_{\nu}\phi$ . The effect of spacetime noncommutativity can be taken into account in the action (2) by replacing the ordinary products in the action with the star products. In curved spacetime, the star product can be expanded as [12]

$$f \star g \equiv \sum_{k=0}^{\infty} \frac{1}{k!} \left( \frac{i}{2} \right)^k \Theta^{\mu_1 \nu_1} \cdots \Theta^{\mu_k \nu_k} \left( D_{\mu_1} \cdots D_{\mu_k} f \right) \left( D_{\nu_1} \cdots D_{\nu_k} g \right), \tag{3}$$

where  $D_{\mu}$  is the covariant derivative. In our consideration, we suppose that the nonzero components of  $\Theta^{\mu\nu}$  are  $\Theta^{12} = -\Theta^{21} = 1/(\Lambda^2 a^2)$ , where a is the cosmic scale factor and  $\Lambda^{-1} = L_s$  is the noncommutative length scale [12].

To study the evolution of density perturbations during inflation, one splits the metric and the inflaton field in the action into the background and the perturbed parts, e.g., for the inflaton field we write  $\phi(\mathbf{x},t) = \phi_0(t) + \delta\phi(\mathbf{x},t)$ . The action for the perturbed field can be obtained by expanding the action (2) around the background. In our consideration the effect of spacetime noncommutativity can be incorporated by just replacing the ordinary product between perturbed variables in the action with the star product. Since we consider the case where  $\Theta^{0i} = 0$ , it follows from eq. (3) that the star product of the background quantity with any field variable is just the ordinary product between functions.

Instead of directly expanding the action (2) around the background, we start from the second order perturbed action for k-inflaton [24, 25],

$$\delta S^{(2)} = \frac{1}{2} \int d^4x a z^2 \left[ \dot{\zeta}^2 + c_S^2 \partial_i \zeta \partial^i \zeta \right], \tag{4}$$

where the dot denotes derivative with respect to time,  $\zeta$  is the curvature perturbation in the comoving gauge,  $z=a(P+\rho)^{1/2}/(c_SH),\ H=\dot{a}/a$  is the Hubble parameter and  $c_S$  is the sound speed, defined by  $c_S^2=P_{,X}/\rho_{,X}$ . Here, the subscript ,X denotes a derivative with respect to X and  $\rho$  is the energy density of the inflaton. Using the relation  $(H/\dot{\phi}_0)\delta\phi=\alpha\delta\phi=\zeta$  between the scalar field perturbation in the uniform curvature gauge and the curvature perturbation in the comoving gauge, the action for the perturbed inflaton field in the uniform curvature gauge can be written as

$$S = \frac{1}{2} \int d^4x a z^2 \alpha^2 \left[ \dot{\delta \phi}^2 + c_S^2 \partial_i \delta \phi \partial^i \delta \phi - \left[ \left( \frac{\dot{a}}{a} + 2 \frac{\dot{z}}{z} \right) \frac{\dot{\alpha}}{\alpha} + \frac{\ddot{\alpha}}{\alpha} \right] \delta \phi^2 \right].$$
 (5)

Replacing the products between the perturbed field variables with the star products, the above action becomes

$$S = S_0 + \delta S_K + \delta S_V + \mathcal{O}\left(\Theta^4\right),\tag{6}$$

where  $\delta S_K$  and  $\delta S_V$  represent the lowest nonzero corrections  $(\mathcal{O}(\Theta^2))$  to the kinetic and potential terms in S respectively. We follow the procedure in [12] to compute the star products in the action (5). The correction to the potential and kinetic terms are then given by

$$\delta S_V = -\frac{m^2}{16} \int d^4 x \frac{az^2 \alpha^2}{\Lambda^4} H^2 \left( \partial_1 \delta \phi \partial^1 \delta \phi + \partial_2 \delta \phi \partial^2 \delta \phi \right), \tag{7}$$

where  $m^2 = (H + 2\dot{z}/z)(\dot{\alpha}/\alpha) + \ddot{\alpha}/\alpha$ 

$$\delta S_K = \frac{1}{16} \int d^4 x \frac{az^2 \alpha^2}{\Lambda^4} H^2 \Big[ \partial_p \partial_0 \delta \phi \partial^p \partial^0 \delta \phi + c_S^2 \partial_p \partial_i \delta \phi \partial^p \partial^i \delta \phi - 2H \partial^p \delta \phi \partial_0 \partial_p \delta \phi + H^2 \partial_p \delta \phi \partial^p \delta \phi \Big], \tag{8}$$

where p=1,2. Expressing the action (6) in terms of the new variable  $v=z\zeta=z\alpha\delta\phi$  and expanding v in Fourier space as

$$v(\mathbf{x},t) = \int \frac{d^3 \mathbf{k}}{(2\pi)^{3/2}} \left( \mathbf{a_k} v_{\mathbf{k}}(t) e^{i\mathbf{k} \cdot \mathbf{x}} + h.c. \right), \tag{9}$$

where  $\mathbf{a_k}, \mathbf{a_k}^{\mathsf{T}}$  satisfy the canonical commutation relations, the action (6), evaluated in the vacuum after normal ordering, becomes

$$S = \int d\eta d^{3}\mathbf{k} \left[ |v'_{\mathbf{k}}|^{2} + \left( \frac{z''}{z} - c_{S}^{2}k^{2} \right) |v_{\mathbf{k}}|^{2} - \frac{H^{2}k_{\perp}^{2}}{8\Lambda^{4}a^{2}} \left( |v'_{\mathbf{k}}|^{2} - c_{S}^{2}k^{2}|v_{\mathbf{k}}|^{2} + \left( \left( \frac{a''}{a} - 2(Ha)^{2} \right) \left( 5 + \frac{\dot{\rho}_{,X}}{H\rho_{,X}} \right) + \frac{z''}{z} \right) |v_{\mathbf{k}}|^{2} \right) \right], \tag{10}$$

where the prime denotes derivative with respect to the conformal time  $\eta = \int da/a$  and  $k_{\perp}^2 = k_1^2 + k_2^2$ . In the above action, we have used  $\rho + P = 2Xc_S^2\rho_{,X}$ . The expression for  $\dot{\rho}_{,X}/(H\rho_{,X})$  in the above action can be simplified, once the model of k-inflation is specified. Hence, in the following consideration we will perform the calculation using a power law k-inflation model. For power law inflation, the scale factor evolves as

$$a \propto t^{\beta},$$
 (11)

where  $\beta$  is a constant parameter, so that  $H = \beta/t$ . From the Friedman equation,  $H^2 = \rho/(3\bar{m}_p^2)$ , one sees that the energy density of power law inflaton evolves as

$$\rho = 3\bar{m}_p^2 \beta^2 \frac{1}{t^2}.$$
 (12)

It follows from the continuity equation,  $\dot{\rho} = -3H(\rho + P)$  and eq. (12), that

$$\Gamma \rho = (\rho + P) = 2XP_{,X},\tag{13}$$

where  $\Gamma$  is constant. Since X and  $c_S$  are constant for the power law k-inflation, one can show that

$$\frac{\dot{\rho}_{,X}}{H\rho_{,X}} = \frac{P_{,X}}{HP_{,X}} = \frac{\dot{\rho}}{H\rho} = -\frac{2}{\beta}.\tag{14}$$

Since  $(\rho + P)^{1/2}$  and H evolve much slower than a during inflation, we suppose that  $z''/z \approx a''/a$ . Using eq. (11), it can be shown that  $a''/a = \beta(2\beta - 1)(1 - \beta)^{-2}/\eta^2$  and  $Ha = \beta/(1-\beta)\eta$ . The action (10) can be written in terms of the variable

$$y_{\mathbf{k}}(\eta) = (1 - \tilde{\epsilon}^2(\eta)k_{\perp}^2)^{1/2}v_{\mathbf{k}}(\eta), \tag{15}$$

where  $\tilde{\epsilon}^2 = H^2/(8\Lambda^4 a^2)$ , up to second order in  $\epsilon$  as

$$S = \int d\eta d^{3}\mathbf{k} \Big[ |y'_{\mathbf{k}}|^{2} - \Big( c_{S}^{2} k_{\mathbf{k}}^{2} - \frac{\beta(2\beta - 1)}{(1 - \beta)^{2} \eta^{2}} + \epsilon^{2} k_{\perp}^{2} \left( 1 - \frac{1}{\beta} + \frac{5}{\beta^{2}} \right) + \mathcal{O}(\epsilon^{4}) \Big) |y_{\mathbf{k}}|^{2} \Big].$$
(16)

Here, we have set  $\epsilon^2 = \tilde{\epsilon}^2 \beta^2/((1-\beta)^2 \eta^2) = H^4/(8\Lambda^4)$ , and have expanded  $\epsilon^2 k_\perp^2/(1-\tilde{\epsilon}^2 k_\perp^2) \approx \epsilon^2 k_\perp^2 + O(\epsilon^4)$ . Let us now make some approximation. For the power law k-inflation model, the relation between the spectral index of the primordial density perturbation and  $\beta$  is  $n_s - 1 = 2/(1-\beta)$ . Hence, using the best fit value of  $n_s$  from the five-year WMAP results, we get  $\beta = 2/(1-0.96) + 1 \approx 51$  and  $\epsilon^2 \propto H^4 \propto 1/\eta^{4/(1-\beta)} \propto \eta^{0.08}$ . Since  $\epsilon^2$  evolves much slower than the third term on the RHS of the action (16), we take  $\epsilon^2$  to be approximately constant. Moreover, for this value of  $\beta$ , we have  $1-1/\beta+5/\beta^2\approx 1.02$ , so that we can set this term equal to one without significantly changing the final result. Using the above approximation, the evolution equation for  $y_{\bf k}$  can be written in the form of the Bessel equation as

$$y_{\mathbf{k}}'' + \left[ c_S^2 k^2 \gamma^2 - \left( \nu^2 - \frac{1}{4} \right) \frac{1}{\eta^2} \right] y_{\mathbf{k}} = 0, \tag{17}$$

where  $\nu = (3/2) + 1/(\beta - 1)$ ,  $\gamma^2 = 1 + \epsilon^2 \sin^2(\theta)/c_S^2$  and  $\sin^2(\theta) = k^2/k_\perp^2$  denotes the angle between the vectors **k** and  $\hat{k}_3$ . Following the standard procedure, the solution of eq. (17) is given by [26]

$$y_{\mathbf{k}} = \frac{\sqrt{\pi}}{2} e^{i(\nu + \frac{1}{2})\frac{\pi}{2}} \sqrt{-\eta} H_{\nu}^{(1)}(-c_S k \gamma \eta), \tag{18}$$

where  $H_{\nu}^{(1)}$  is the Hankel function of the first kind. The argument of the Hankel function can be written as

$$-c_S k \gamma \eta \approx -c_S k \eta \left( 1 + \frac{1}{2} \frac{\epsilon^2 \sin^2(\theta)}{c_S^2} \right) = \xi + \delta \xi, \tag{19}$$

where  $\delta \xi$  denotes a small contribution from  $\epsilon^2 \sin^2(\theta)/2c_S^2$ . We expand the Hankel function around  $\xi$  as

$$H_{\nu}^{(1)}(-c_S k \gamma \eta) \simeq H_{\nu}^{(1)}(\xi) + \frac{dH_{\nu}^{(1)}(\xi')}{d\xi'} \Big|_{\xi} \delta \xi$$

$$= H_{\nu}^{(1)}(\xi) + \left(\nu H_{\nu}^{(1)}(\xi) - H_{\nu+1}^{(1)}(\xi)\xi\right) \frac{\delta \xi}{\xi}.$$
(20)

Since we are interested in the long wavelength perturbation modes, we express the hankel function in the asymptotic form [26],

$$H_{\nu}^{(1)}(\xi \ll 1) \sim \sqrt{2/\pi} e^{-i\frac{\pi}{2}} 2^{\nu - \frac{3}{2}} \frac{\Gamma(\nu)}{\Gamma(3/2)} \xi^{-\nu},$$
 (21)

so that the curvature perturbation is given by

$$\zeta_{\mathbf{k}} = \frac{v_{\mathbf{k}}}{z} \simeq e^{i(\nu - \frac{1}{2})\frac{\pi}{2}} 2^{(\nu - \frac{3}{2})} \frac{\Gamma(\nu)}{\Gamma(3/2)} \times \frac{(-c_S k \eta)^{\frac{1}{2} - \nu}}{z(\eta)\sqrt{2c_S k}} \left(1 - \nu \frac{\epsilon^2 \sin^2(\theta)}{2c_S^2}\right), \tag{22}$$

and finally we obtain the primordial power spectrum

$$\mathcal{P}_{\mathbf{k}}^{\zeta} = \left[ 2^{\frac{2}{\beta - 1}} \left| \frac{\Gamma(\nu)}{\Gamma(3/2)} \right|^2 \left( \frac{\beta - 1}{\beta} \right)^{\frac{2\beta}{\beta - 1}} \right] \frac{GH_1^2}{\pi} c_S^{\frac{1 + \beta}{1 - \beta}} \times$$

$$\beta \left( \frac{k}{k_1} \right)^{\frac{2}{1 - \beta}} \left( 1 - \nu \frac{\epsilon^2 \sin^2(\theta)}{c_S^2} \right),$$

$$= A_s(\beta, c_S) \left( \frac{k}{k_1} \right)^{\frac{2}{1 - \beta}} \left( 1 - \nu \frac{\epsilon^2 \sin^2(\theta)}{c_S^2} \right),$$
(23)

where the subscript 1 denotes the evaluation at the time when the wavenumber  $k_1$  crosses the horizon. It can be seen that the obtained power spectrum is direction-dependent due to the spacetime noncommutativity. The magnitude of the noncommutative contribution depends on the angle between the vectors  $\mathbf{k}$  and  $k_3$ , and also depends on the sound speed for the k-inflation. Neglecting the contributions from spacetime noncommutativity, the above power spectrum gives rise to the usual power spectrum as in [24].

#### 3. The CMB constraints

In this section, we will constrain the contributions from spacetime noncommutativity on CMB anisotropies using the CMB data. It is well known that if the primordial power spectrum is direction-dependent, the statistics of CMB will become anisotropic, i.e., the two-point function of the temperature fluctuations is no longer rotationally invariant. Here, we consider only the two-point function because we assume the non-Gaussianity of the CMB fluctuations to be negligible. In addition to spacetime noncommutativity, the direction-dependent primordial power spectrum can also be a consequence of many phenomena in the early universe, for example see [27] - [28]. To compare theoretical prediction with the observation, it is convenient to expand the temperature anisotropy into spherical harmonics

$$\Delta T(\hat{n}) = T(\hat{n}) - T_0 = \sum_{l,m} a_{lm} Y_{lm}(\hat{n}) , \qquad (24)$$

where  $T_0$  is the mean temperature of the CMB. If we write the direction-dependent primordial power spectrum as [27, 22]

$$\mathcal{P}(\mathbf{k}) = A(k) \left[ 1 + \sum_{LM} g_{LM} Y_{LM}(\hat{k}) \right], \tag{25}$$

the covariance matrix of  $a_{lm}$  will be

$$\langle a_{l_1 m_1} a_{l_2 m_2}^* \rangle = \delta_{l_1 l_2} \delta_{m_1 m_2} C_{l_1} + \sum_{l, M} \Xi_{l_2 m_2 L M}^{l_1 m_1} D_{l_1 l_2}^{L M}. \tag{26}$$

Here,  $C_{l_1}$  is the CMB angular power spectrum, given by

$$C_{l_1} = (4\pi)^2 \int_0^\infty dk \, k^2 A(k) [T_{l_1}(k)]^2, \tag{27}$$

where  $T_{l_1}$  is the CMB transfer function which is taken to be rotationally invariant. It is known that if the two-point function of the temperature anisotropy is not rotationally invariant, the covariance matrix of  $a_{lm}$  will not be diagonal. The off diagonal elements of the covariance matrix appear in the second term of eq. (26) This term is given by

$$D_{l_1 l_2}^{LM} = (4\pi)^2 (-i)^{l_1 - l_2} \int_0^\infty dk \, k^2 A(k) g_{LM} T_{l_1}(k) T_{l_2}(k), \tag{28}$$

and

$$\Xi_{l_1 m_1 l_2 m_2}^{l_3 m_3} = \sqrt{\frac{(2l_1 + 1)(2l_2 + 1)}{4\pi (2l_3 + 1)}} \mathfrak{C}_{l_1 0 l_2 0}^{l_3 0} \mathfrak{C}_{l_1 m_1 l_2 m_2}^{l_3 m_3},\tag{29}$$

where  $\mathfrak{C}_{l_1m_1l_2m_2}^{l_3m_3}$  are the Clebsch-Gordan coefficients. Comparing the power spectrum in eq. (25) with the one in eq. (23), we find that the non zero components of  $g_{LM}$  are

$$g_{00} = -\frac{4\sqrt{\pi}}{3} \frac{\nu \epsilon^2}{c_s^2}$$
 and  $g_{20} = \frac{4}{3} \sqrt{\frac{\pi}{5}} \frac{\nu \epsilon^2}{c_s^2}$ . (30)

We see that the contributions from spacetime noncommutativity also influence the diagonal elements of the covariance matrix, i.e. they modify the amplitude of  $C_l$ . Substituting  $g_{LM}$  from eq. (30) into eq. (26), we obtain the covariance matrix

$$\langle a_{l_1m_1} a_{l_2m_2}^* \rangle \simeq C_{l_1} \left\{ \delta_{l_1 l_2} \delta_{m_1 m_2} \left[ 1 + \frac{\nu \epsilon^2}{c_S^2 (2l_1 + 1)} \times \left( \frac{(l_1 + 1)^2 - m_1^2}{2l_1 + 3} + \frac{l_1^2 - m_1^2}{2l_1 - 1} - 1 \right) \right] - \left( \delta_{l_1 - 2l_2} \delta_{m_1 m_2} \frac{\nu \epsilon^2 C_{l_1 l_2}}{c_S^2 (2l_1 - 1)} \times \right.$$

$$\left. \sqrt{\frac{((l_1 - 1)^2 - m_1^2)(l_1^2 - m_1^2)}{(2l_1 - 3)(2l_1 + 1)}} + l_1 \leftrightarrow l_2 \right) \right\},$$
(31)

where  $C_{l_1 l_2} = (4\pi)^2 \int_0^\infty dk k^2 A(k) T_{l_1}(k) T_{l_2}(k) / C_{l_1}$ .

We next constrain the contributions from spacetime noncommutativity in this covariance matrix using the five-year WMAP foreground-reduced maps [30]. Since the spacetime noncommutativity also influences the diagonal elements of the covariance matrix and  $\epsilon \propto H^2$ , we use eq. (23) to write the contribution from spacetime noncommutativity as

$$\frac{3\epsilon^2}{2c_S^2} \simeq A_s^2 \Sigma,\tag{32}$$

where  $A_s$  is the amplitude of the primordial power spectrum and

$$\Sigma \simeq \frac{3}{16} \left(\frac{\pi}{G\beta}\right)^2 L_s^4 c_S^{\frac{4}{\beta-1}}.$$
 (33)

In the above two equations, we have used  $\beta \gg 1$ . We adopt the procedures in [19] to compute the posterior probability of the parameters  $\Sigma$  and  $A_s$ , given the observed temperature anisotropies  $\mathbf{a}$ ,

$$P(\bar{\sigma}|\mathbf{a}) \propto L(\mathbf{a}|\bar{\sigma})P(\bar{\sigma}),$$
 (34)

where  $\bar{\sigma} = \Sigma$ ,  $A_s$  is the set of parameters,  $L(\mathbf{a}|\bar{\sigma})$  is the likelihood and  $P(\bar{\sigma})$  is the prior. Since the galactic contamination cannot be completely removed from some regions of the sky, one does not have the full-sky CMB maps with well-defined error properties. To reduce the galactic contamination, one masks the contaminated regions as

$$c_i = M_i \Delta T_i, \tag{35}$$

where i is the pixel index,  $c_i$  is the masked CMB map,  $\Delta T_i$  is the full-sky map and  $M_i$  is a mask which is zero at the contaminated points and is one elsewhere. The above relation can be written in harmonic space as

$$c_{lm} = M_{lm,l'm'}b_{l'm'},$$
 (36)

where the matrix  $M_{lm,l'm'}$  is given by

$$M_{lm,l'm'} = \sum_{LM} M_{LM} \Xi_{LMl'm'}^{lm}.$$
 (37)

Here,  $c_{lm}$ ,  $M_{lm}$  and  $b_{lm}$  are the spherical harmonic coefficients of  $c_i$ ,  $M_i$  and  $\Delta T_i$  respectively. Moreover, due to the instrument noise, the finite beams resolution and the discreteness of the temperature maps, the contributions to the unmasked CMB map come from the sum of the instrument noise with the convolution between the signal of the CMB anisotropies and the window function, such that

$$\Delta T = W\mathbf{a} + \mathcal{N},\tag{38}$$

where W is the window function and  $\mathcal{N}$  is the instrument noise. We suppose that the contributions from the beam and the pixel asymmetries are negligible. Using eqs. (36) and (38), the covariance matrix of the masked temperature multipoles can be written as

$$C_{lm,l'm'} = \sum_{l_1m_1l_2m_2} M_{lm,l_1m_1} \Big[ W_{l_1} \langle a_{l_1m_1} a_{l_2m_2}^* \rangle W_{l_2} + N_{l_1m_1,l_2m_2} \Big] M_{l_2m_2,l'm'}^*, (39)$$

where  $N_{l_1m_1,l_2m_2}$  is the pixel noise covariance matrix, given by

$$N_{l_1 m_1, l_2 m_2} = \Delta a \sum_{LM} \Xi_{LM l_2 m_2}^{l_1 m_1} N_{LM}. \tag{40}$$

Here,  $\Delta a$  is the area of each pixel in the temperature map, and  $N_{LM}$  is defined as

$$N_{LM} = \sum_{i} \Delta a \frac{\sigma_0^2}{n_i^{\text{obs}}} Y_{LM}(\hat{r}_i), \tag{41}$$

where  $\sigma_0$  is the rms noise of a single observation and  $n_i^{\text{obs}}$  is the number of observations of pixel i.

In order to compute the likelihood, the inversion of the covariance matrix is required. Since the inversion of the large matrix is time consuming, we avoid to inverse the large covariance matrix by writing the likelihood function in terms of the reduced bipolar coefficients instead of  $c_{lm}$ . The reduced bipolar coefficients are defined as [18]

$$A_{LM} = \sum_{l_1 m_1 l_2 m_2} (-1)^{m_2} d_{l_1 m_1} d_{l_2 m_2}^* \mathfrak{C}_{l_1 m_1 l_2 - m_2}^{LM}, \tag{42}$$

where  $d_{lm}$  are the harmonic coefficients of the temperature anisotropies. For the full-sky and noiseless case, the mean of the reduced bipolar coefficients for the noncommutative k-inflation can be computed using eq. (31), and the non zero components are

$$\langle A_{00} \rangle = \sum_{l} (-1)^{l} C_{l} \sqrt{2l+1} \left( 1 - \frac{2}{3} A_{s}^{2} \Sigma \right),$$

$$\langle A_{20} \rangle = -2 A_{s}^{2} \Sigma \sum_{l} (-1)^{l} C_{l} \sqrt{\frac{l(l+1)(2l+1)}{45(2l-1)(2l+3)}}$$

$$-2 A_{s}^{2} \Sigma \sum_{l \geq l} (-1)^{l} C_{l} \sqrt{\frac{2l(l-1)}{15(2l-1)}}.$$

$$(44)$$

In the more realistic case, the mask and the instrument noise must be taken into account, so that the reduced bipolar coefficients are computed from  $c_{lm}$  in eq. (36) and their mean is

$$\langle A_{LM} \rangle = \sum_{l_1 l_2 m_1 m_2} (-1)^{m_2} C_{l_1 m_1, l_2 m_2} \mathfrak{C}_{l_1 m_1 l_2 - m_2}^{LM}. \tag{45}$$

It can be seen from the above equation that due to the effect of the mask,  $\langle A_{00} \rangle$  and  $\langle A_{20} \rangle$  will not be the only non zero components of  $\langle A_{LM} \rangle$ .

We define

$$\delta A_{LM} = A_{LM} - \langle A_{LM} \rangle, \tag{46}$$

and write the covariance matrix for  $\delta A_{LM}$  as

$$\langle \delta A_{LM} \delta A_{L'M'}^* \rangle = C_{LM,L'M'}$$

$$= \sum_{l_1 m_1 l_2 m_2} \sum_{l_3 m_3 l_4 m_4} \mathfrak{C}_{l_1 m_1 l_2 m_2}^{LM} \mathfrak{C}_{l_3 m_3 l_4 m_4}^{L'M'}$$

$$\times \left( C_{l_1 m_1, l_3 m_3} C_{l_2 m_2, l_4 m_4} + C_{l_1 m_1, l_4 m_4} C_{l_2 m_2, l_3 m_3} \right). \tag{47}$$

Therefore, the posterior probability function takes the form

$$P(\bar{\sigma}|A_{LM}) \propto \frac{\exp\left(-\frac{1}{2}Z^{2}\right)}{\det^{1/2}C}P(A_{s})$$

$$Z^{2} = \sum_{LML'M'} \delta A_{LM} \left(C^{-1}\right)_{LM,L'M'} \delta A_{L'M'}^{*}.$$
(48)

Here, we have used a flat prior on  $\Sigma$  and a Gaussian prior on  $A_s$ . For the Gaussian prior, the mean and variance of  $A_s$  are taken from the five-year WMAP results [33]. Since the contributions from spacetime noncommutativity mainly appear in the  $\langle A_{00} \rangle$  and  $\langle A_{20} \rangle$ , we restrict the multipole index L of  $A_{LM}$  to be less than 4. We note that the parallel computing of covariance matrices  $C_{l_1m_1,l_2m_2}$  and  $C_{LM,L'M'}$  can be easily implemented in the Healpix package [31]. The data that are used to computed  $\delta A_{LM}$  are the fiveyear WMAP foreground-reduced V2 and W1 differential assembly temperature maps [30]. These maps are masked using the band-limited masks in [19]. According to [19], we limit the multipole index of  $c_{lm}$  and  $M_{LM}$  to be  $l \leq 62$  and  $L \leq 92$  respectively. The covariance matrix  $\mathcal{C}$  can be computed from the covariance matrix in eq. (26). Since the spacetime noncommutativity does not affect the cosmic evolution after the inflationary epoch, we can use CMBEASY [32] to compute the CMB transfer function and  $c_l$  by supposing that the cosmic evolution after inflation obeys the  $\Lambda$ CDM model whose parameters are taken from the best fit value of the five-year WMAP results [33]. However, recall that the amplitude of the primordial power spectrum is treated as a free parameter. We compute the posterior probability function for  $\bar{\sigma}$  and marginalize it over  $A_s$  to obtain the marginalized posterior probability function for  $\Sigma$ . The marginalized posterior probability functions for  $\Sigma$  obtained from V2 and W1 maps have a peak at negative  $\Sigma$ , i.e. negative  $c_S^2$ . However we restrict ourselves to the case where  $c_S^2 > 0$ , so that the confidence intervals for  $\Sigma$  can be obtained from the areas under the curves of The marginalized posterior probability functions in figure 1.

Since the parameters  $\beta$  and  $c_S$  cannot be constrained using the above analysis, the upper bound for the noncommutative length scale  $L_s$  can be computed from the upper bound for  $\Sigma$  if the values of  $\beta$  and  $c_S$  are specified. For simplicity, we suppose that the values of  $\beta$  and  $c_S$  are known precisely, so that the upper bound for  $L_s$  can be written as  $L_s < 1.4 \times 10^4 \beta^{1/2} c_S^{1/(1-\beta)}/m_p \text{Gev}^{-1} \sim 1.4 \times 10^{-28} \beta^{1/2} c_S^{1/(1-\beta)}$  cm at 99.7% confidence level. Here,  $m_p$  is the Planck mass. It can be seen that if inflaton evolves more slowly, the upper bound for  $L_s$  will increase and the dependence of this upper bound on  $c_S$  becomes weaker. We note that  $\beta$  is the inverse of the slow-roll parameter. As shown in [24], the ratio of the tensor to scalar perturbations amplitudes r depends on  $c_S$ . We roughly estimate the values of  $\beta$  and  $c_S$  using the values of  $n_s$  and r from the five-year WMAP results, and obtain  $L_s < 10^{-27} \text{cm}$  at 99.7% confidence level.

	68%CL	95%CL	99.9%CL
W1	0.024	0.048	0.070
V2	0.029	0.055	0.78

**Table 1.** The upper bound for the parameter  $\Sigma \times 10^{18}$  from W1 and V2 maps.

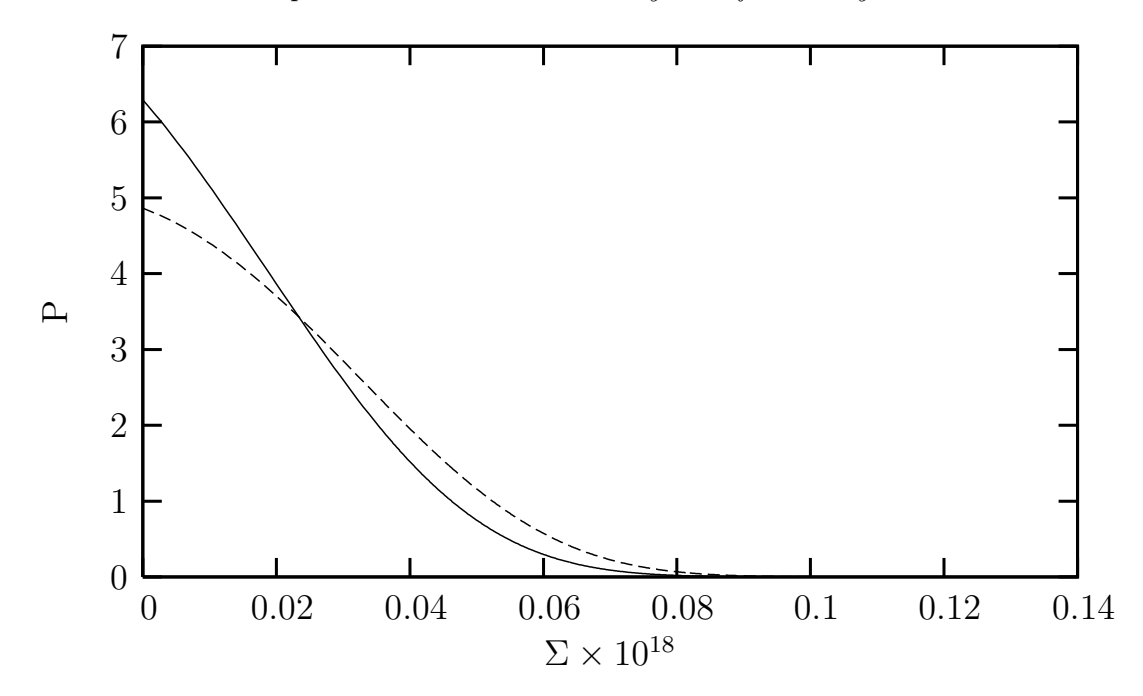


Figure 1. The marginalized posterior probability functions for  $\Sigma$ . The solid line represents the probability function from W1 map, while the long dashed line represents the probability function from V2 map. Here,  $\Sigma$  is restricted to be positive.

#### 4. Conclusions

In this work, we study the effect of spacetime noncommutativity on the rotational invariance of the primordial power spectrum, and constrain the contributions from this effect using CMB data. For the power law k-inflation model, the deviation from rotational invariance of the primordial power spectrum due to the spacetime noncommutativity effect depends on the factor  $\nu H_1^4 L_s^4/(8c_S^2)$ . This result will give rise to the result in [12] if  $c_S = 1$ , and will be invalid if the Hubble parameter does not evolve sufficiently slow during inflation.

Since the primordial power spectrum is direction-dependent in our consideration, the covariance matrix for the harmonic coefficients of the CMB temperature anisotropies has off diagonal elements. In our case, these off diagonal elements arise from the spacetime noncommutativity contributions. As is well known, this implies that statistics of the CMB anisotropies become anisotropic. The spacetime noncommutativity also contributes to the diagonal elements of the covariant matrix suggesting that the noncommutative contribution also modifies the amplitude of the CMB angular power spectrum.

Both contributions from spacetime noncommutativity are simultaneously constrained using five-year WMAP foreground-reduced V2 and W1 maps. The upper bound for the ratio  $L_s c_S^{1/(\beta-1)}/\beta^{1/2}$  is approximately  $1.4 \times 10^{-28} \mathrm{cm}$  at 99.7% confidence level. If we suppose that the values of  $\beta$  and  $c_S$  are known precisely, the upper bound for the noncommutative length scale can be written as  $L_s < 1.4 \times 10^{-28} \beta^{1/2} c_S^{1/(1-\beta)} \mathrm{cm}$  at 99.7%

confidence level. This shows that if inflaton evolves more slowly, the upper bound for  $L_s$  will increase and the dependence of this upper bound on  $c_S$  becomes weaker. Estimating the values of  $\beta$  and  $c_S$  using the best fit cosmological parameters from the five-year WMAP results, we obtain  $L_s < 10^{-27} \text{cm}$  at 99.7% confidence level.

#### Acknowledgments

The author would like to thank T. Souradeep for instructive conversations, and A. Ungkitchanukit for comments on the manuscript. He would also like to thank P. Wongjun for his checking of some parts of the calculations. He acknowledges the use of the Legacy Archive for Microwave Background Data Analysis (LAMBDA) and HEALPix package. This work is supported by Thailand Research Fund (TRF).

#### References

- [1] Guth A H, The inflationary universe: a possible solution to the horizon and flatness problems, 1981 Phys. Rev. **D23** 347
- [2] Linde A D, A new inflationary universe scenario: a possible solution of the horizon, flatness, homogeneity, isotropy and primordial monopole problems, 1982 Phys. Lett. **B108** 389
- [3] Albrecht A and Steinhardt P J, Cosmology for grand unified theories with radiatively induced symmetry breaking, 1982 Phys. Rev. Lett. 48 1220
- [4] Komatsu E et al, Five-year Wilkinson Microwave Anisotropy Probe (WMAP) observations: cosmological interpretation, 2009 Astrophys. J. Suppl. 180 330 [arXiv:0803.0547]
- [5] Brandenberger R H and Martin J, The robustness of inflation to changes in superPlanck scale physics, 2001 Mod. Phys. Lett. A16 999 [arXiv:astro-ph/0005432]
- [6] Martin J and Brandenberger R H, The transplanckian problem of inflationary cosmology, 2001 Phys. Rev. D63 123501 [arXiv:hep-th/0005209]
- [7] Szabo R J, Quantum field theory on noncommutative spaces, 2003 Phys. Rept. **378** 207 [arXiv:hep-th/0109162]
- [8] Seiberg N and Witten E, String theory and noncommutative geometry, 1999 JHEP 9909 032 [arXiv:hep-th/9908142]
- [9] Brandenberger R and Ho Pei-Ming, Noncommutative space-time, stringy space-time uncertainty principle, and density fluctuations, 2002 Phys. Rev. **D66** 023517 [arXiv:hep-th/0203119]
- [10] Tsujikawa S, Maartens R and Brandenberger R H, Noncommutative inflation and the CMB, 2003 Phys. Lett. B574 141 [arXiv:astro-ph/0308169]
- [11] Huang Qing-Guo and Li M, CMB power spectrum from noncommutative space-time, 2003 JHEP 0306 014 [arXiv:hep-th/0304203]
- [12] Lizzi F, Mangano G, Miele G and Peloso M, Cosmological perturbations and short distance physics from noncommutative geometry, 2002 JHEP 0206 049 [arXiv:hep-th/0203099]
- [13] Fang K, Chen B and Xue W, Non-commutative geometry modified non-gaussianities of cosmological perturbation, 2008 Phys. Rev. D77 063523 [arXiv:0707.1970]
- [14] Akofor E, Balachandran A P, Jo S G, Joseph A and Qureshi B A, Direction-dependent CMB power spectrum and statistical anisotropy from noncommutative geometry, 2008 JHEP 0805 092 [arXiv:0710.5897]
- [15] Cai Yi-fu and Piao Yun-Song Probing noncommutativity with inflationary gravitational waves, 2007 Phys. Lett. **B657** 1 [arXiv:gr-qc/0701114]
- [16] Akofor E, Balachandran A P, Joseph A, Pekowsky L and Qureshi B A, Constraints from CMB on spacetime noncommutativity and causality violation, 2008 [arXiv:0806.2458]

- [17] Armendariz-Picon C, Footprints of statistical anisotropies, 2006 JCAP **0603** 002 [arXiv:astro-ph/0509893]
- [18] Hajian A and Souradeep T, Testing global isotropy of three-year Wilkinson Microwave Anisotropy Probe (WMAP) data: temperature analysis, 2006 Phys. Rev. **D74** 123521 [arXiv:astro-ph/0607153]
- [19] Armendariz-Picon C and Pekowsky L, Bayesian limits on primordial isotropy breaking, 2009 Phys. Rev. Lett. 102 031301 [arXiv:0807.2687]
- [20] Groeneboom N E and Eriksen H K, Bayesian analysis of sparse anisotropic universe models and application to the 5-yr WMAP data, 2009 Astrophys. J. 690 1807 [arXiv:0807.2242]
- [21] Hajian A and Souradeep T, Measuring statistical isotropy of the CMB anisotropy, 2003 Astrophys. J. 597 L5 [arXiv:astro-ph/0308001]
- [22] Pullen A R and Kamionkowski M, Cosmic microwave background statistics for a direction-dependent primordial power spectrum, 2007 Phys. Rev. D76 103529 [arXiv:0709.1144]
- [23] Armendariz-Picon C, Damour T and Mukhanov V F, K-inflation, 1999 Phys. Lett. **B458** 209 [arXiv:hep-th/9904075]
- [24] Garriga J and Mukhanov V F, Perturbations in k-inflation, 1999 Phys. Lett. **B458** 219 [arXiv:hep-th/9904176]
- [25] Chen X, Huang Min-xin, Kachru S and Shiu G, Observational signatures and non-Gaussianities of general single field inflation, 2007 JCAP 0701 002 [arXiv:hep-th/0605045]
- [26] Riotto A, Inflation and the theory of cosmological perturbations, 2002 Trieste 2002, Astroparticle physics and cosmology 317 [arXiv:hep-ph/0210162]
- [27] Ackerman L, Carroll S M and Wise M B, Imprints of a primordial preferred direction on the microwave background, 2007 Phys. Rev. D75 083502 [arXiv:astro-ph/0701357]
- [28] Boehmer C G and Mota D F, CMB anisotropies and inflation from non-standard spinors, 2008 Phys. Lett. **B663** 168 [arXiv:0710.2003]
- [29] Koivisto T S and Mota D F, Vector field models of inflation and dark energy, 2008 JCAP 0808 021 [arXiv:0805.4229]
- [30] Hinshaw G et al, Five-Year Wilkinson Microwave Anisotropy Probe (WMAP) observations: data processing, sky maps, and basic results, 2009 Astrophys. J. Suppl. 180 225 [arXiv:0803.0732]
- [31] Gorski K M, Hivon E, Banday A J, Wandelt B D, Hansen F K, Reinecke M and Bartelman M, HEALPix – a framework for high resolution discretization, and fast analysis of data distributed on the sphere, 2005 Astrophys. J. 622 759 [arXiv:astro-ph/0409513]
- [32] Doran M, CMBEASY:: an object oriented code for the Cosmic Microwave Background, 2005 JCAP 0510 011 [arXiv:astro-ph/0302138]
- [33] Dunkley J et al, Five-Year Wilkinson Microwave Anisotropy Probe (WMAP) observations: likelihoods and parameters from the WMAP data, 2009 Astrophys. J. Suppl. 180 306 [arXiv:0803.058]